中 國 醫 藥 大 學
臨 床 醫 學 研 究 所
博 士 學 位 論 文

CAPON 調控心臟再極化：臨床證據與分子機轉

CAPON Modulates Cardiac Repolarization: Clinical Evidence and Molecular Mechanisms

指 導 教 授：蔡輔仁 教 授
共同指導教授：李英雄 教 授
共同指導教授：黃秋錦 教 授

研 究 生：張 坤 正

中 華 民 國 九 十 九 年 七 月

誌　謝

心臟電氣生理學的醫療、教學與研究，最終的目標是能融會貫通基礎與臨床的知識，這是我個人一直努力的方向，三年來，在中國醫藥大學臨床醫學研究所的學習，讓我在這個領域稍有進展，內心充滿感恩。

首先我要感謝，啟發與教導我走入臨床電生理領域的老師：吳德朗教授、葉森洲教授與陳宇清醫師，他們的教導，讓我具備了臨床電生理的知識與技術，才能在因緣際會下跟隨洪瑞松教授回母校發展，期間有幸與黃水坤教授共事，並蒙其推薦於 2005 年 4 月至美國 Johns Hopkins University，跟隨細胞電生理大師 Eduardo Marban 教授學習 molecular genetics 與 patch clamp，Dr. Marban 充分支持與指導，讓我的心臟電氣生理知識正式跨入細胞層次。在 2007 年 7 月回國後，承蒙李英雄教授、蔡輔仁教授、黃秋錦教授與藍先元所長協助與指導，才能在繁忙的醫療業務下，規劃研究方向，逐步往前邁進。我更要感謝中國醫療體系蔡董事長、林正介院長，一路的支持與提拔，讓我有機會赴美國進修與就讀臨床醫學研究所，實現夢想。

最後，我要感謝父母的栽培，我的內人張淑文與我的女

兒張瑀倫的支持與包容，讓我無後顧之憂，才能全力以赴完成學業。

張坤正謹誌於

中國醫藥大學臨床醫學研究所

民國九十九年七月

目　錄

目　錄 — 圖

目　錄 — 表

中文摘要

CAPON 是 1998 年首度在腦組織發現的蛋白，具有調節 nNOS 產生 NO 的重要功能。2006 年 4 月，一項由美國約翰霍普金斯大學及德國慕尼黑大學主導的大規模人類基因體 SNP association study，發表在 Nature Genetics 雜誌，此研究首度發現 CAPON 的基因變異會影響心臟再極化，反應在心電圖 QT interval 的變化。由於 QT interval 太長或太短，皆容易造成心因性猝死，因此，這項研究結果具有幾項重大意義，值得進一步探討：第一、CAPON 可能是一項引起心因性猝死的嶄新危險因子；第二、CAPON 本身並非離子通道蛋白，但卻能影響心臟離子通道的功能；第三、CAPON-nNOS-target protein-NO 之訊息作用途徑在心臟生理或病理狀況下，扮演重要的角色。但 CAPON 究竟在心臟扮演何種角色，它又如何影響心臟再極化，過去一無所知，我們從研究 CAPON 是否在心臟表達著手，再探討 CAPON 與 NOS1 的蛋白交互作用，並利用腺病毒作載體研究 CAPON 透過與 NOS1 的交互作用，當基因過度表達時，會抑制鈣離子通道電流，並進而縮短心肌細胞再極化的時間，經由此研究的結果可以印證人類族群 CAPON 基因變異和 QT 長短具有相關性的發現。然而，我們認為另有三大問題，急需解答：CAPON 基因變異對國人心電圖 QT interval 的影響，當心臟處在病理狀態下 CAPON 扮演何種角色，及 CAPON

如何調控心臟電氣與收縮功能之交互作用。

針對第一個問題，我們假設 CAPON 基因變異確實會影響國人心電圖 QT interval，這種影響可以反應在健康的個人，或當個人接受可引起 QT 延長的藥物治療時，帶有 CAPON 基因變異者可能進一步延長其 QT interval，我們的策略是: 基因鑑定一群海洛因（heroin）成癮正在接受 methadone 治療的成年男女，初期測試兩個重要的 CAPON SNP，rs10494366 與 rs1415263，來看帶有基因變異者是否在服用 methadone 前、後影響其心電圖 QT interval。關於這個假設，在精神分裂患者服用 risperidone 治療的族群（58 人）上，我們初步發現帶有 rs1415263 homozygous T alleles 者，在接受 risperidone 治療後其心電圖 QTc interval 由 396.7±26.7 ms 延長為 403.3±20.6 ms（Δ6.7 ms），而帶有 CC（407.7±29.8 ms vs. 397.7±17.4 ms）與 CT alleles（401.0±17.1 ms vs. 394.5±18.2 ms）者在服用 risperidone 後 QTc interval 反而下降，而 rs10494366 這個在三大歐美族群研究皆會造成 QTc 延長的 SNP，初步看來並不影響這個特定台灣精神分裂族群服用 risperidone 前、後的 QTc interval。基於這個初步結果，促成我們想進一步探討藥癮患者在接受 methadone 治療的過程，帶有 CAPON 基因變異是否會造成嚴重 QTc 延長，引發致命性心室不整脈而導致猝死。

另外，我們也計畫以大鼠急性或亞急性心肌梗塞的模式去探討

CAPON 在心肌梗塞部位與正常心肌表達是否不同，並且使用單一心肌細胞研究 CAPON 表達量不同時，對於心臟電氣與收縮功能之交互作用（excitation-contraction coupling）的影響。

在第一章，我們回顧心肌細胞膜上各種離子電流決定心電圖 QT 長短的機轉，說明研究 QT 的重要性，目前 congenital long QT syndrome 的分類，探討影響 QT 之大型 genome-wide association study，藉由過去所知 CAPON 在神經系統的作用，並進而研究 CAPON 在心臟所扮演的角色。

在第二章中，在研究 CAPON 的分子機轉方面，我們利用腺病毒作載體以 *in vivo* gene transfer 的方式，將 CAPON 過度表達，探討 CAPON 的生理功能；在臨床研究 CAPON 變異與心電圖 QT 相關性方面，我們鑑定 24 項常見的 CAPON 基因變異，分析心電圖的 QTc 在單純 methadone 影響下與 methadone 加基因變異影響下的相關性。

在第三章中，在 CAPON 的分子機轉方面，我們呈現 CAPON 影響心臟再極化的分子機轉，另外我們也引用其他機構新近發表之心肌梗塞動物模式以探討 CAPON 之角色功能；在臨床證據方面，我們提出 methadone 或 methadone 加 CAPON 基因變異對心電圖 QTc 的影響的結果。

第四章，著重於討論現有 CAPON 分子機轉與臨床研究的結果，

並和過去相關的研究作比較，以規劃進一步研究的方向，並舉出現有研究的限制。

第五章，則說明經由這些研究成果，可以讓我們從臨床證據與分子機轉全面釐清 CAPON 在心臟生理與病理狀況下所扮演的角色，確定 CAPON 基因變異對國人接受 methadone 治療之特定族群心臟再極化的影響，特別是，是否會造成嚴重 QTc 延長，引發致命性心律不整，進而有助於防治心因性猝死。

關鍵詞：QTc、心臟再極化、猝死、藥癮、methadone。

Abstract

Congenital long or short QT syndrome caused by gene mutations is well recognized as capable of predisposing to ventricular tachycardia and sudden cardiac death. Apart from the rare disease-causing mutations, common genetic variants in a neuronal nitric oxide synthase (NOS1) regulator, CAPON gene, have recently been associated with QT interval variations in a human whole-genome SNP association study in 2006; this association has been replicated in two different Caucasian populations in 2007. We have recently identified CAPON expression and interaction with NOS1-NO pathways to modulate cardiac repolarization in the heart, which provides the rationale for the association of CAPON gene variants and extremes of QT interval in Caucasian populations. However, there are at least three important issues remaining to be answered. Firstly, the association of CAPON gene variants and extremes of QT interval has not been documented in non-Caucasian populations; secondly, the role of CAPON in cardiac repolarization is not clear in pathological or diseased model, and lastly, CAPON-mediated modulation of excitation-contraction coupling has not been investigated.

To answer the first question, we hypothesize that CAPON gene

variants affect healthy Taiwan Chinese population and the CAPON gene variants cause further QTc prolongation if the subjects are on QT-prolonging drugs. Our strategies are to genotype two important candidate SNPS, rs10494366 and rs1415263, in a heroin-addicted "healthy" Taiwan Chinese population who are undergoing methadone (a QT-prolonging drug via blocking I_{Kr}) treatment to assess the effects of gene variants on the pre- and the post-treatment QTc intervals. This approach is based on our preliminary data from a schizophrenic population (n=58). We found that when the schizophrenic patients carry the TT alleles at rs1415263, they tended to have QTc prolongation after receiving risperidone (another QT-prolonging drug via blocking I_{Kr}) treatment (396.7±26.7 ms vs. 403.3±20.6 ms), while those bearing the CC or CT alleles did not. Interestingly, rs1419263, a highly significant SNP associated with QTc prolongation in Caucasians did not affect the QT interval in this Taiwanese population both before and after risperidone treatment.

With the findings, we are motivated to investigate the influence of CAPON gene variants on the development of QTc prolongation and potential lethal ventricular tachyarrhythmias in a drug-addicted Taiwan

Chinese population undergoing methadone treatment. This study might enable us to identify a novel genetic risk factor for life-threatening ventricular tachyarrhythmias occurring in this particular population while undergoing methadone treatment and lead to development of new therapeutic interventions to prevent sudden cardiac death.

In chapter 1, we stress the importance of studying QT interval and the underlying ionic mechanisms responsible for QTc prolongation. In addition to the well-known congenital long QT syndrome, Arking et al. has identified a new genetic marker, CAPON (NOS1AP), as a novel QT modifier in a recent genome-wide association study. This finding was soon replicated and confirmed by 3 other studies in different populations. As CAPON was previously unexpected to play a role in the heart, we designed an animal study to explore the molecular functions of CAPON in the heart. Additionally, we wanted to know whether the particular CAPON gene variants are also associated QTc prolongation in a Taiwanese population.

In chapter 2, we used *in vivo* gene transfer technique to overexpress CAPON in guinea pig heart then exploring the cellular electrophysiological remodeling after CAPON overexpression with and

without pharmacological intervention. For the CAPON gene variants and QTc association study, we genotyped 24 CAPON single nucleotide polymorphisms (SNPs) using a high throughput SNP array technique in a heroin addiction population undergoing methadone treatment. We wanted to answer the effects of CAPON gene variants on the QTc with and without methadone.

In chapter 3, we found the expression of CAPON protein in the heart and when CAPON is overexpressed, it interacts with NOS1-NO pathway to affect the $I_{Ca,L}$ and I_{Kr} currents causing acceleration of cardiac repolarization (shortening of action potential duration). The electrophysiological remodeling of CAPON could be reversed by L-NAME, attesting the mechanistic link of CAPON to NOS1-NO pathway. In clinical part, we found low maintenance dose of methadone is associated with QTc prolongation and methadone-associated QTc prolongation appears to be gender-dependent. In this study, men appear to be more susceptible than women to methadone associated QTc prolongation. For the CAPON SNP association study, we found rs10918594 C>G, CAPON variant but not rs10494366 T>G is associated QTc prolongation in this Taiwanese population and use of methadone in

patients with rs10918594 homozygous variant might potentiate the QTc prolongation.

In chapter 4, we discussed the molecular mechanisms by which CAPON modulated cardiac repolarization and pointed out several potential limitations of the basic study. Indeed, future studies, particularly using a CAPON knock-out model are necessary to further elucidate CAPON function in the heart. For the clinical study, it seems that rs10918594 C>G is also associated QTc prolongation in this Taiwanese population, yet it needs to be confirmed in a larger population study and the underlying mechanisms of gender-dependent susceptibility of methadone associated QTc prolongation needs to be explored.

In chapter 5, we conclude that CAPON is a new QT modifier in the heart which exists not only in the western population but likely also in Aisan population. Therefore, people carrying the genetic variants might be at a greater risk of developing serious ventricular tachyarrhythmias and sudden death when superimposed with additional long QT conditions, such as drugs and/or electrolytes imbalance.

Keywords: QTc, cardiac repolarization, sudden death, drug-addiction, methadone

第一章　前言

第一節　研究背景

心電圖的 QT interval 是指從心電圖的 QRS 波起點到 T 波結束的時間，以 msec 表示，這段期間被用來代表心臟之再極化時間，而 QT interval 也相當於心室細胞完成一個動作電位的時間，當心室細胞去極化，使得細胞膜上的電位差上升達到閾值，帶正電的鈉離子電流（I_{Na}）大量的湧入細胞內，使得膜電位上升到最高點，接著帶正電的鉀離子電流（I_{to}）流向細胞外，使心肌細胞迅速再極化，此短暫迅速的再極化，又因帶正電的鈣離子（I_{Ca}）電流湧入細胞內而趨緩，接著帶正電的鉀離子電流（I_K）向細胞外流出，使細胞完成再極化，並由 I_{K1} 維持靜止膜電位的穩定。

爲什麼要研究心電圖 QT interval？從過去的研究顯示，不論是健康者或罹患疾病族群（例如糖尿病或冠心病），QT interval 延長都是引發心因性猝死的一個重要指標，所以值得深入研究。而我們已知大約 30％的 QT interval 是由基因決定，所以不管在先天或後天 long QT syndrome，基因因素都扮演著關鍵的角色，以先天性 long QT syndrome 而言，從 1957 年第一病例被證實是由基因突變引起後，至今 50 年來，已經陸續發現 12 型之先天性 long QT syndrome（表 1），除了第 4（Ankyrin-B）、第 11（AKAP9, Yotiao）與第 12（SNTA1, α-1 Syntrophin）

型是由於調控離子通道之蛋白發生突變以外，其餘皆由離子通道蛋白本身突變導致。而臨床上第 1 至第 3 型的 long QT syndrome 病例占 99%以上，在心電圖的 phenotype 方面，第 1 型的 long QT syndrome 具有寬大的 T 波，第 2 型具有小而分叉型之 T 波，而第 3 型具有較長之 ST 波段及小而尖型之 T 波，即便 genotype 陽性的患者，其 QTc 的長短與是否發生過暈厥或心因性猝死，仍是決定病人預後與選擇何種治療的重要指標，過去研究顯示，如果 QTc 小於 500 msec 並且從未發生過暈厥，其 5 年內發生心因性猝死的機會，只有 0.5%，但若 QTc 大於 500 msec，或過去曾發生過急救，則 5 年內發生心因性猝死的機會高達 14%，然而，臨床上仍有高達 30%以上的病人身上找不到這些已知的的 long QT syndrome 的基因突變，再者，一些藥物或電解質異常的 long QT syndrome 病例，這些傳統的 long QT 基因突變也無法完全解釋其 long QT phenotype，由於這些限制，便掀起了大型的基因研究，試圖來找尋新型影響 QT interval 的基因變異。

表 1：最新先天性 Long QT Syndrome 的分類。

Congenital Long QT Syndrome

Genetics of Long QT Syndrome（LQTS）

LQT Type	Gene	Chromosome Locus	Ion Channel	Effects	Percent of LQTS
Autosomal-dorminant（Romano-Ward）					
LQT1（1991）	KCNQ1（KVLQT1）	11p15.5	α- subunit of I_{Ks}	↓ I_{Ks}	50 %
LQT2（1994）	KCNH2（HERG）	7q35-36	α- subunit of I_{Kr}	↓ I_{Kr}	45 %
LQT3（1994）	SCN5A	3p21-24	α- subunit of I_{Na}	↑ I_{Na}	3-4 %
LQT4（1995）	Ankyrin-B	4q25-27			＜1 %
LQT5（1997）	KCNE1（minK）	21q22.1-22.2	β- subunit of I_{Ks}	↓ I_{Ks}	＜1 %
LQT6（1999）	KCNE2（MiRP1）	21q22.1-22.2	β- subunit of I_{Kr}	↓ I_{Kr}	＜1 %
LQT7（2001）	KCNJ2	17q23	Kir2.1	↓ I_{K1}	＜1 %
Autosomal-recessive（Jervell and Lange-Nielsen）					
JLN1	KCNQ1（KVLQT1）	11p15.5	α- subunit of I_{Ks}	↓ I_{Ks}	＜1 %
JLN2	KCNE1（minK）	21q22.1-22.2	β-subunit of I_{Ks}	↓ I_{Ks}	＜1 %

LQT8:CACNA1C（Timothy syndrome）--- $Ca_v1.2$
LQT9: Caveolin-3---↑ late I_{Na}
LQT10:SCN4B--- ↑ late I_{Na}
LQT11: AKAP9, Yotiao--- ↓ I_{Kr}
LQT12: SNTA1, α-1 Syntrophin--- ↑ late I_{Na}

在 2006 年 4 月，一項由美國約翰霍普金斯大學及德國慕尼黑大學主導的大規模人類基因體 SNP association study，發表在 Nature Genetics 雜誌，此研究首度發現 CAPON 的基因變異會影響心臟再極化，反應在心電圖 QT interval 的變化。此研究是在德國 KORA 所進行，第一階段是篩選 QTc 最常與最短的 7.5 percentile，作 genome-wide association study（GWA），找出最顯著差別的基因變異（SNP），再進行第二階段的測試，QTc 兩個極端各 300 人，再選出最有顯著差異的

SNPs，進行第三階段 3400 人的分析，意外找出 CAPON 是一影響心電圖 QTc 的全新基因。

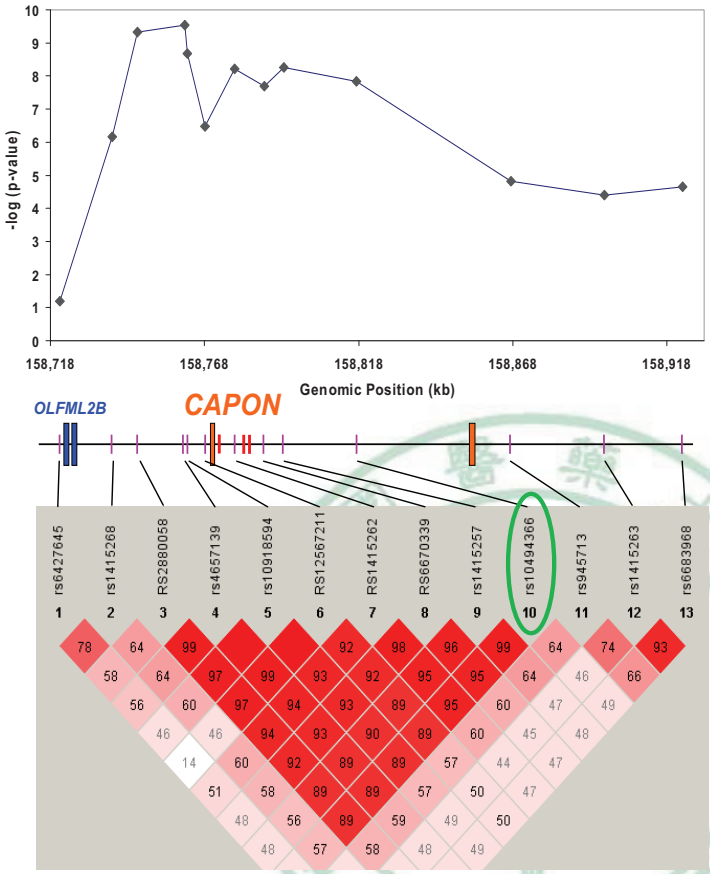

圖 1：Arking et al. 首度利用 genome-wide association study 發現 CAPON 和 QTc 延長的相關性。

第二節　研究目的

緊接著在這第一個 GWA 發表後，陸續有幾個重要的 replication 研究，首先是 2007 年針對美國 old order Amish 族群的相關性研究，發現 CAPON rs10494366(T/G)的基因變異跟 QTc 延長有顯著相關，接著同年在荷蘭鹿特丹的研究，也顯示 CAPON 基因變異 rs10494366

及 rs10918594 與 QTc 延長有顯著的相關性，在 2008 年歐裔美國人糖尿病家族的研究，更進一步證實 CAPON 基因變異 rs10494366 及 rs10918594 與 QTc 延長有非常顯著的相關性，由以上不同族群的研究顯示 rs10494366 與 QTc 延長的相關性最為顯著（圖 2）。

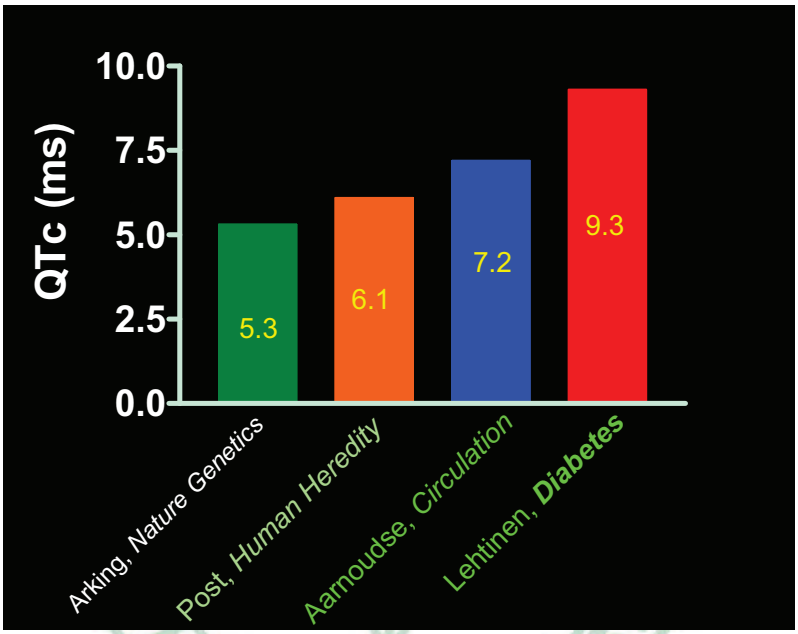

圖 2：rs10494366 homozygote 與 QTc 延長，4 個大型相關性研究之比較。

這些史無前例基因研究的結果，大大的挑戰我們過去對於 QT 生理的認識。

CAPON 於 1998 年首度於大鼠的腦神經組織被發現，是一個高度 conserved 的蛋白，大鼠與人類的 CAPON 蛋白約有 92%胺基酸序列是相似的，CAPON 蛋白具有一個 amino-terminus phospho-tyrosine binding（PTB）domain 和一個 carboxyl-terminus 的 PDZ binding

domain，在腦組織 CAPON 可以透過和 PDZ domain 的鍵結，和 PSD95 競爭與 NOS1 的結合，進而使 NMDA-NOS1-NO 的訊息傳遞路徑受到抑制，CAPON 可以說是 NOS1 的 regulator 和 adaptor，可以把 NOS1 帶到標的蛋白進行特定的生理作用（圖 3），儘管如此 CAPON 是否也在心臟扮演類似的角色，在當時一無所知。

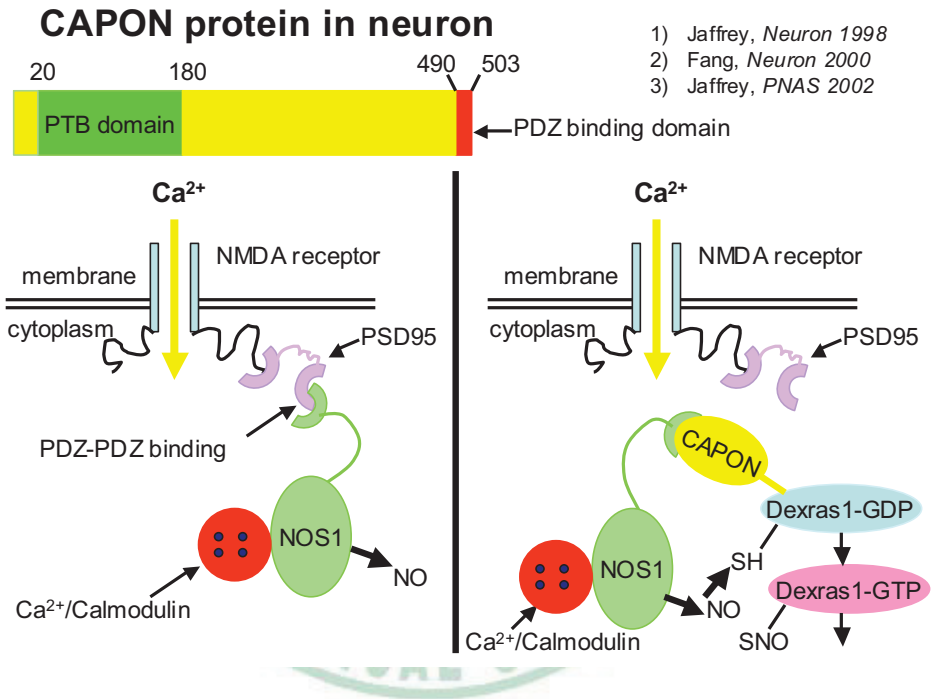

圖 3：Jaffery et al. 首度發現 CAPON 在神經細胞扮演重要功能。

NOS1 與 NOS3 兩者在心肌細胞皆呈現組成性表達，NOS1 可和細胞膜上的 Na^{+}-K^{+} ATPase 與 Ca^{2+}/calmodulin-dependent Ca^{2+} ATPase (PMCA)交互作用，在內質網（sarcoplasmatic reticulum，SR）NOS1 在結構上與 ryanodine receptor 2（RyR2）及 cardiac SR Ca^{2+} ATPase（SERCA2）緊密結合，以調節細胞內的鈣循環及興奮-收縮互動

（excitation-contraction coupling），在使用基因轉殖鼠將 NOS1 過度表達的實驗顯示 NOS1 會和細胞膜上的 L-type 鈣離子通道結合並且抑制 L-type 鈣離子電流（$I_{Ca,L}$），這些證據顯示 NOS1 在心臟生理扮演重要角色，因此我們假設 CAPON 也在心臟表達並且透過 NOS1 進行生理作用，因此我們首先從在心臟找尋內生性的 CAPON 蛋白開始，並且利用腺病毒載體進行 *in vivo* 基因導入的方式將 CAPON 過度表達來探討 CAPON 所扮演的生理角色，並進而研究 CAPON 與 NOS-NO 訊息路徑的交互作用。

在了解了 CAPON 在心臟的分子機轉後，我們也進行臨床研究探討常見的 CAPON 基因變異（SNPs）是否與國人 QTc 延長具有相關性。

第二章　研究方法

第一節　基礎研究

Cloning of CAPON cDNA, Plasmid Construction, and Adenovirus Preparation. Total RNA was extracted from the ventricular myocardium of adult guinea pig with an RNEasy mini kit (Qiagen) according to the manufacturer's instructions and then quantified by a UV spectrometer. Total RNA (2 mg) was subjected to a 20.5-ml reverse transcriptase reaction to synthesize cDNA after the SuperScript II first-strand cDNA synthesis protocol (Invitrogen). The full-length CAPON cDNA was cloned and amplified by PCR using the first-strand cDNA as template with a forward primer of 5'-ACCATGCCCAGCAAAACCAAGTAC-3' and a reverse primer of 5'-CTACACGGCGATCTCATCAT-3'. The CAPON cDNA PCR product was inserted into pTOPO (Invitrogen) plasmid to generate pTOPO-CAPON, according to the manufacturer's protocol. The CAPON cDNA was then cut out of pTOPO-CAPON from the NsiI restriction enzyme site and ligated with the compatible PstI site in the multiple cloning sites of AdCIG plasmid to generate the adenoviral plasmid, pAdCMV-CAPON-IRES-GFP, capable of coexpressing GFP as a reporter. The construction of the adenoviral plasmid was verified by

multiple restriction enzymes digestion testing and DNA sequencing. Adenovirus vectors (AdCAPON-GFP) were produced by Cre-lox recombination of purified y5 viral DNA and shuttle vector DNA as described in previously. Overexpression of CAPON protein was confirmed by Western blotting and immunofluorescent staining. The recombinant viral products were plaque-purified, expanded, and then purified to generate the concentration in the order of 10^{10} pfu/ml.

Western Blot Analysis. Fresh ventricular myocardium and brain and lung tissues were harvested from adult guinea pig and rapidly frozen in liquid nitrogen and stored at -80°C for further processing. The preparation and quantification of the frozen protein tissues have been described. Briefly, the tissue samples were homogenized in a 4′ volume of RIPA buffer (Sigma-Aldrich) plus complete protease inhibitors (Roche). The protein concentration was determined by Lowry assay. Each protein sample was heated in SDS sample buffer and loaded on a 4-12% gradient Bistris Nu-PAGE gel (Invitrogen). Proteins were transferred to polyvinylidene difluoride (Bio-Rad) or nitrocellulose membrane (Invitrogen) in transfer buffer without SDS. According to the experimental purposes, blots were probed with primary antibodies,

including a rabbit polyclonal antibody against the C terminus of CAPON (sc-9138, 1:200-1:1,000 dilution; Santa Cruz Biotechnology), a mouse monoclonal anti-NOS1 antibody (sc-5302, 1:200 dilution; Santa Cruz Biotechnology), or a rabbit polyclonal anti-NOS3 antibody (sc-654, 1:200 dilution; Santa Cruz Biotechnology), respectively, and detected by SuperSignal West Femto chemiluminescent reagents (Pierce) with an anti-rabbit (sc-2004; Santa Cruz Biotechnology) or anti-mouse (GE Healthcare) secondary antibody coupled to horseradish peroxidase. To verify CAPON bands, blots were also probed with a goat polyclonal antibody against the N-terminal epitope (2-14 aa) of CAPON (ab3928, 1:200-1:1,000 dilution; abcam) for comparison. For GAPDH normalization, blots were incubated in the stripping buffer containing 62.5 mM Tris×HCl (pH 6.7), 2% SDS, and 100 mM b-mercaptoethanol at 50°C for 30 min, followed by reacting with a mouse monoclonal antibody to GAPDH (Fitzgerald Industries International, Inc.) and visualized by using SuperSignal West Pico chemiluminescent agents (Pierce) with an anti-mouse secondary antibody (GE Healthcare). For protein samples from the culture ventricular myocytes, the GAPDH was probed by a goat polyclonal antibody (IMG-3073, 1:15,000 dilution; IMGENEX,) and

detected by SuperSignal West Femto chemiluminescent substrates (Pierce) with an anti-goat secondary antibody (sc-2020; Santa Cruz Biotechnology).

Coimmunoprecipitation of CAPON and Nitric Oxide Synthase (NOS). The rabbit anti-CAPON antibody (sc-9138; Santa Cruz Biotechnology) or the rabbit anti-NOS1 antibody (sc-648; Santa Cruz Biotechnology) was bound and immobilized to a protein G support with cross-linking agent (DSS) according to the manufacturer's instructions (Pierce). The tissue homogenates from normal guinea pig ventricular myocytes were immunoprecipitated overnight with the antibody-protein G complex at 4°C. After an extensive wash, the immunoprecipitated antigens were then eluted and became the samples for Western blotting. To prepare the sample for Western blot analysis, 5 ml of sample buffer (Pierce) was added to a 20-ml elution sample and boiled at 100°C for 5 min before SDS/PAGE. To probe NOS1, NOS3, and CAPON, the blots were reacted with the monoclonal mouse anti-NOS1 antibody (sc-5302; Santa Cruz Biotechnology), the rabbit polyclonal anti-NOS3 antibody (sc-654; Santa Cruz Biotechnology), and the rabbit anti-CAPON antibody (sc-9138; Santa Cruz Biotechnology), respectively, and then detected

with SuperSignal West Femto chemiluminescent reagents with corresponding secondary antibodies. For control experiments, the ventricular myocardial homogenates were incubated overnight with antibody-free protein G complex and then processed in the same ways for Western blot analysis.

Cell Culture and Adenovirus Transduction. HEK293 cells (American Type Culture Collection) maintained in DMEM (Invitrogen) with 10% FBS (Invitrogen) and 1% penicillin/streptomycin (Invitrogen) were seeded at ~50% confluence in T25 flasks (Salsdect) and cultured in a 5% CO_2 and 37°C environment. Cells were transduced with 10 ml of AdCAPON-GFP at 80% confluence and cultured for 48 h to ensure adequate transgenic expression. Cells were then harvested, lysed, homogenized, and subjected to Western blotting as described above. A T25 flask of HEK293 cells of same confluence without viral transduction was used as a control. For myocytes culture, the freshly isolated ventricular myocytes dispersed in DMEM with 5% FBS and 1% penicillin/streptomycin were plated into 6-well culture dishes precoated with laminin and cultured for 1 h to let cells attach to the bottoms of the culture dishes. Then, the medium was replaced with fresh medium, and

cells were infected with ~10^8 pfu/ml AdCAPON-GFP or AdGFP or not infected with either virus and cultured for 2 days. After that, cells were harvested for Western blot analysis. To compare the NOS1 level in freshly isolated ventricular myocytes, when the cells became attached to the bottoms of the culture dishes 1 h after plating, the medium was replaced with AdCAPON-GFP-containing or noncontaining DMEM, and then the cells were harvested immediately for protein analysis, which was designated as 0 h of cell culture.

Immunofluorescent Staining and Confocal Microscopic Imaging. Freshly isolated guinea pig ventricular myocytes were attached to coverslips precoated with laminin, fixed in 4% paraformaldehyde, and then permeabilized with 0.2% Triton X-200. After blocking with 10% normal goat serum, the myocytes were reacted overnight with the rabbit polyclonal anti-CAPON antibody (sc-9138, 1:50-1:100 dilution; Santa Cruz Biotechnology) at 4°C, followed by a Texas red-conjugated anti-rabbit secondary antibody (sc-2780; Santa Cruz Biotechnology). Background fluorescence caused by unspecific binding of the secondary antibody was estimated by omitting preincubation with primary CAPON antibody in a subset of myocytes. Nuclear counterstaining was carried out

by using a DNA-specific dye, Hoechst 33342 (Molecular Probes). Ventricular myocytes were examined by a laser scanning confocal microscope with multiple track techniques (LSM510; Zeiss). Texas red was excited by helium/neon laser (543 nm), GFP by argon laser (488 nm), and Hoechst by diode UV laser (405 nm).

In Vivo Gene Transfer and Myocyte Isolation. Adult guinea pigs (weight, 300-400 g) were anesthetized with 4% isoflurane, intubated, and supported by a ventilator with a maintenance isoflurane dose of 1.5-2% during the operation. The guinea pigs then underwent open-chest intramyocardial injection of the adenoviral vectors, 2×10^{10} pfu/ml AdCAPON-GFP, or 3×10^{10} pfu/ml AdGFP into the left ventricular apex with a total volume of 200 ml by using 30-gauge needle as described. The ventricular myocytes were isolated 72 h after *in vivo* gene transfer, typically within 3-5 days, with standard techniques. The transduced ventricular myocytes were judged by their vivid green fluorescence by using a xenon arc lamp at 488/530 nm (excitation/emission).

Electrophysiological and Pharmacological Studies. Experiments were performed by using whole-cell patch clamp technique with an Axopatch 200B amplifier (Axon Instruments) while sampling at 10 kHz

for current recordings or 2 kHz for voltage recordings and filtering at 2 kHz. Pipettes had tip resistances of 2-4 MW when filled with internal solutions. All recordings were performed at 33 ±1°C, but I_{Na} was recorded at room temperature (22°C). Cells were superfused with a physiological saline solution containing 140 mmol/liter NaCl, 5 mmol/liter KCl, 2 mmol/liter $CaCl_2$, 1 mmol/liter $MgCl_2$, 10 mmol/liter Hepes, and 10 mmol/liter glucose; the pH was adjusted to 7.4 with NaOH. The pipette solution was comprised of 100 mmol/liter potassium aspartate, 20 mmol/liter KCl, 1 mmol/liter $MgCl_2$, 5 mmol/liter Hepes, 5 mmol/liter EGTA, 5 mmol/liter MgATP, and adjusted to pH 7.3 by KOH. Action potentials were elicited continuously by brief suprathreshold depolarizing current pulses at 1, 2, and 0.05 Hz until steady state was reached. APD was measured as the time from overshoot to 10% (APD_{10}), 25% (APD_{25}), 50% (APD_{50}), 75% (APD_{75}), and 90% repolarization (APD_{90}). For I_{K1} and total I_K recordings, 10 mM nitrendipine (Sigma-Aldrich) was added to the external solution to block calcium currents. For separation of I_{Kr} and I_{Ks}, after recordings of the total I_K, cells were exposed to 30 mM chromanol 293B (Aventis Pharma) to fully suppress the I_{Ks} and to obtain the remaining I_{Kr}. For measurement of $I_{Ca,L}$, the external solution contained

128 mmol/liter NaCl, 10 mmol/liter CsCl, 1 mmol/liter $MgCl_2$, 10 mmol/liter NaHepes, 2 mmol/liter $CaCl_2$, adjusted to pH 7.4 by HCl; and the pipette solution consisted of 110 mmol/liter CsCl, 0.5 mmol/liter $MgCl_2$, 10 mmol/liter Hepes, 20 mmol/liter tetraethylammonium chloride (TEA-Cl), 5 mmol/liter BATPA, 5 mmol/liter MgATP, adjusted by pH 7.2 by CsOH. To measure $I_{Ca,L}$, the I_{Na} was steady-state-inactivated by a prepulse from -80 to -40 mV, and the membrane potential was held at -40 mV throughout the recordings. I_{Na} was recorded by using symmetrical 10 mmol/liter Na^+ with external solution containing 10 mmol/liter NaCl, 2 mmol/liter $MgCl_2$, 5 mmol/liter CsCl, 120 mmol/liter TEA-Cl, 20 mmol/liter Hepes, adjusted to pH 7.4 by NaOH; the internal solution contained 10 mmol/liter NaCl, 140 mmol/liter CsCl, 10 mmol/liter Hepes, adjusted to pH 7.2 by CsOH.

Because CAPON is a regulator and adaptor of NOS1, to understand the role of the NOS-NO pathway in CAPON overexpression-mediated electrophysiological changes is mechanistically important. For this purpose, freshly isolated ventricular myocytes from the same animal were divided into two fractions; fraction 1 was pretreated with 1 mM L-N^G-nitro-L-arginine methyl ester (L-NAME) (Sigma-Aldrich) for 30

min before the patch clamp study and then continuously exposed to the same concentration of L-NAME in the bath solution throughout the study, whereas fraction 2 was not exposed to L-NAME for comparison.

Intracellular NO Imaging with DAR-4M AM. DAR-4M AM (AXXORA) is a membrane-permeable rhodamine-based chromophore, capable of detecting intracellular NO as low as 7 nM. When incubated with cells, it enters the cells because of the presence of the acetoxymethyl ester (AM) moiety. Once inside the cells, the AM moiety is hydrolyzed by cytoplasmic esterase to form the membrane-impermeable DAR-4M. When NO is produced intracellularly, DAR-4M can react with it to form a triazole compound, DAR-4MT. DAR-4MT is a stable, membrane-impermeable, and fluorescent compound that can be visualized with a fluorescent microscope with rhodamine filter. For chromophore loading, freshly isolated ventricular myocytes dispersed in DMEM without phenol red (GIBCO) were incubated with 10 mM DAR-4M AM in 35-mm glass-bottom culture dishes (P35G-0-14-C; MatTek Corporation) for 30 min at room temperature or incubated at 37°C with the addition of 2 mM L-arginine (Sigma-Aldrich) for 60 min. After incubation, the extracellular chromophore was carefully washed

away by DMEM without phenol red three times. The cells were then subjected to confocal microscopic imaging by using an LSM510 system with an excitation wavelength of 543 nm and emission wavelength of 560 nm to image the NO fluorescent marker in CAPON-overexpressing ventricular myocytes and control myocytes. The fluorescent intensity was quantified by LSM510 software. L-NAME (2 mM) and sodium nitroprusside (1 mM; Sigma-Aldrich) were used to inhibit or enhance the NO fluorescent marker to verify the specificity of NO detection by DAR-4M AM chromophore.

第二節　臨床研究

Study Subjects Evaluation

Between September 2008 and May 2010, consecutive heroin dependence patients admitted to outpatient methadone clinics of the Division of Addiction Psychiatry of China Medical University Hospital, Taichung, TAIWAN were recruited for the study. The diagnosis of opioid dependence was according to DSM-IV criteria made by a specialist in psychiatry. Eligible male or female patients who had opioid addiction history of more than 1 year should be aged ≧18 and ≦65 years with

good physical health determined by complete physical examination, laboratory tests, and a 12-lead ECG screening for entry of the study. To be eligible, patients or their reliable caregivers are being expected to ensure acceptable compliance and visit attendance throughout the study period. Patients were excluded from the study if they are currently with severe physical and mental disorders including an uncontrolled and/or clinically significant cardiac, hepatic or renal dysfunction as well as premorbid mental retardation or multiple substances dependence that would compromise patient safety or preclude study participation. Women of childbearing potential, not using adequate contraception as adjusted by investigators or not willing to comply with contraception for the duration of the study and females who are pregnant or nursing were also excluded from the study. The Institutional Review Board for the Protection of Human Subjects at China Medical University Hospital approved this study protocol. At baseline (immediately before methadone induction), a complete medical history, physical examination and laboratory tests were obtained. Each individual subject gave a signed informed consent before inclusion. Recent drug and alcohol use was assessed by patient report. Particular attention was given to screen for medications affecting cardiac

conduction, repolarization, or methadone metabolism. All patients received a 20 mg starting dose of oral methadone followed by subsequent 10 mg incremental increases. Doses were titrated to maintenance levels based on self-reported heroin use, presence of opioid withdrawal symptoms, and urine toxicology evidence of illicit opioid abuse. A standard digital 12-lead electrocardiography (ECG) (GE Healthcare, USA) was performed when the participants underwent stable methadone maintenance treatment program, typically ≥ 1 month after initiation of methadone. In laboratory, urine toxicology assays for illicit opioids and amphetamines were performed at regular intervals during the study. The psychiatric evaluation tools consisted of Mini International Neuropsychiatric Inventory (MINI) and Structured Clinical Interview for DSM-IV, Addiction severity index (ASI) and Tridimensional Personality Questionnaire (TPQ) for a comprehensive patient assessment and care.

Electrocardiographic Measurements

All 12-lead ECGs were recorded by a GE Marquette's MAC 5500 ECG recorder (GE Medical Systems, Milwaukee, WI, USA), using a standardized protocol with special attention to precise localization of each electrode. A 10-second resting 12-lead ECG recorded at a sampling

frequency of 500 Hz and was digitally transmitted and stored to the MUSE system (GE Marquette) at the core ECG laboratory of China Medical University Hospital for subsequent analysis. All the stored ECGs were visually inspected by an experienced cardiologist blinded to the study to exclude those with technical errors and inadequate quality before being processed for automatic measurement by the 2001 version of the Marquette 12SL program (GE Marquette). The machine-read QT interval measurements were based on a "Global Median" beat, a superimposition of 12 representative median beats. The 12SL measures the earliest onset of the Q wave in any lead and the latest offset of the T wave in any lead to derive the QT interval which was then corrected by heart rate (QTc) using Bazett's formula ($QTc=QT/RR^{1/2}$). The 12SL algorithm includes the U wave in the QT measurement if the U wave merges with the preceding T wave. Otherwise, the U wave is excluded from the QT measurement. A 12-lead ECG was obtained when the subjects were receiving stable maintenance methadone treatment, typically one month after the initiation of methadone. The ECG recording was performed after observed intake of individual participant's daily methadone. To study the cross sectional association between oral methadone doses and QTc duration, all eligible

ECGs from subjects undergoing maintenance methadone therapy were used. In a subset of participants, ECGs were obtained before, 1 month and 3 months after the initiation of methadone therapy to assess the chronological changes of the QTc intervals. ECGs with a wide QRS duration of ≥ 120 ms caused by complete right or left bundle-branch block, ventricular preexcitation, or intraventricular conduction delay were excluded from analyses. In addition, we also exclude ECGs with atrial fibrillation and evidence of myocardial infarction to avoid potential non-methadone influence on the QT intervals. Similarly, other confounding factors that might affect the QT duration at the time of ECG recording including the concomitant use of any other QT-altering drugs, electrolyte imbalance with hypokalemia or hypocalcemia are excluded from analyses.

In laboratory, urine toxicology assays for illicit opioids and amphetamines will be perform at regular intervals during the study and blood samples will collect to extract DNA before initiation of methadone.

1. Inclusion criteria

Patients must meet all of these inclusion criteria to be eligible for enrollment into the study:

A. Capacity and willingness to give written informed consent

B. A diagnosis of opioid dependence according to DSM-IV criteria made by a specialist in psychiatry

C. Male or female patient aged ≧18 and ≦65 years

D. Good physical health determined by complete physical examination, laboratory tests, and EKG

E. Patient or a reliable caregiver can be expected to ensure acceptable compliance and visit attendance for the duration of the study.

2. Exclusion criteria

The presence of any of the following will exclude a patient from study enrollment:

A. Current evidence of an uncontrolled and/or clinically significant medical condition, e.g., cardiac, hepatic and renal failure that would compromise patient safety or preclude study participation.

B. Premorbid mental retardation

C. Current Other major Axis-I DSM-IV diagnosis other than opioid dependence such as multiple substance dependence

D. Increase in total SGOT, SGPT, gamma-GT, BUN and creatinine by more than 3X ULN (upper limit of normal)

E. Women of childbearing potential, not using adequate contraception as per investigator judgment or not willing to comply with contraception for the duration of the study.

F. Females who are pregnant or nursing.

3. Evaluation tools

A. Mini International Neuropsychiatric inventory (MINI) and Structured Clinical Interview for DSM-IV: for psychiatric disorder evaluation and diagnosis

B. Addiction severity index (ASI): evaluation of substance related family, physical, occupational, legal, economical factors

C. *Tridimensional Personality Questionnaire (TPQ)*: Self rating scale, TPQ, will be used as an instrument to investigate the personality trait of the patient with opioid dependence. The Chinese version of the TPQ used in the present study is a 100-item, self-administered, true–false instrument. Consisting of two subscales, the Cronbach's α of the novelty-seeking subscale (NS) was 0.70, and that of the harm-avoidance subscale (HA) was 0.87. Since the reward dependency (RD) dimension has no adequate reliability among Han Chinese in Taiwan, only NS and HA dimensions will be

analyzed in this study.

DNA extraction and genotyping

We will obtain DNA from the participants via blood by phlebotomy. DNA will be extracted from blood samples using standard procedures. All samples will be obtain on 9 A.M. before and after 6 weeks of treatment and 10 ml blood will be obtain. After extracting of DNA and mRNA of blood mononuclear cells, the sample will be storage under -80℃. Genotyping of the two candidate SNPs of CAPON, rs10494366 and rs1415263, will be performed by using 1 ng genomic DNA extracted from leukocytes, as previously reported.

DNA extraction, amplification, and mutation screening:

Total genomic DNA was extracted from 10 to 15 ml of venous blood from each participant after informed consent was obtained. DNA was purified from lymphocyte pellets according to standard procedures using a Puregene kit (Gentra Systems, Minneapolis, MN) or the phenol-chloroform extraction method. Twenty-four SNPs spanning the non-coding region of CAPON gene were identified using GenBank database. Multiplex PCR and SNP analyses were performed with the GenomeLab SNPstream genotyping platform (Beckman Coulter Inc.

Fullerton, CA) and its accompanying SNPstream software suite. The primers for the multiplex PCR and single base extension primers were optimally designed by Web-based software provided at Beckman Coulter Inc. PCR primers were designed to amplify a short stretch of DNA (90 bp) that encompasses the SNP of interest. The tagged extension primers used to identify the SNPs were designed in two parts. The 5' portion of the probe is complementary to one of 12 unique single stranded DNA oligonucleotides that are microarrayed at a specific location within each well of a 384-well microplate. The 3' portion of the probe is complementary and precisely adjacent to the SNP, which enables detection of the presence of either or both nucleotides of the SNP through the incorporation of a fluorescent-labeled terminating nucleotide. Twelve-plex PCR reactions were performed in 384-well plates (MJS BioLynx, Brockville, ON) in a 5 μl volume using 6 ng of DNA, 75 μM dNTPs, 0.5 U of AmpliTaq Gold (Perkin-Elmer, Wellesley, MA), and the 24 PCR primers at a concentration of 50 nM each in 1 X PCR buffer. Thermal cycling was performed in GeneAmp PCR system 9700 thermal cyclers (Applied Biosystems, Foster City, CA) using the following program: initial denaturation at 95 °C for 5 min followed by 40 cycles of

95 °C for 30 s, 50-55 °C for 55 s, 72 °C for 30 s. After the last cycle, the reaction was held at 72 °C for 7 min. Following PCR, plates were centrifuged briefly and 3 μl of a mixture containing 0.67 U Exonuclease I (Amersham Pharmacia, Buckinghamshire, UK) and 0.33 U shrimp alkaline phosphatase (Amersham Pharmacia) were added to each well. The plates were sealed and incubated for 30 min at 37 °C and at 95 °C for 10 min. The tagged extension primers were extended with single TAMRA- or bodipy-fluorescein-labeled nucleotide terminator reactions and then spatially resolved by hybridization to the complementary oligonucleotides arrayed on the 384-well microplates (SNPware Tag array). The Tag array plates were imaged with a two-laser, two-color charged couple de- vice-based imager (GenomeLab SNPstream array imager). The 12 individual SNPs were identified by their position and fluorescent color in each well according to the position of the tagged oligonucleotides. Sample genotype data were generated on the basis of the relative fluorescent intensities for each SNP and computer processed for graphical review. PCR was performed on 50 ng of genomic DNA with a GeneAmp PCR system 9700 thermocycler (Applied Biosystems). The Touchdown PCR cycling condition was performed as follows: initial

preheating step for 11 min at 95 °C to achieve a hot start, followed by 12 cycles of 94 °C for 20 s, 68 °C for 20 s, and 72 °C for 45 s, the annealing temperature decreased 0.5 °C per cycle until 62 °C; followed by 30 cycles of 94 °C for 20 s, 62 °C for 20 s, and 72 °C for 45 s; with a final elongation at 72 °C for 10 min. Amplified PCR products were separated by agarose gel electrophoresis and visualized by staining with ethidium bromide. They were then purified in purification columns (QIAquick; Qiagen, Valencia, CA) and sequenced using dye terminator chemistry (BigDye Terminator ver. 3.1 on a model 3100 Genetic Analyzer; Applied Biosystems, Foster City, CA). Sequences were trimmed for quality and aligned using BioEdit software (version 5.0.6). Normal and affected individual DNA sequences were aligned to the known reference genomic sequence (GenBank NT_011362), available via the National Center for Biotechnology Information (NCBI) database and compared for sequence variation.

第三節　統計方法

Statistical Analysis

All continuous variables are expressed as mean ± SD and all categorical variables are expressed as count (percentage). Two-sample t test, paired t test and chi-square test were used to perform univariate comparison. Pearson's correlation, simple and multiple regression models were used to assess the association between QTc intervals and methadone doses. All analyses were performed for male and female separately. The variables in the model included age, gender, methadone doses, age at exposure to heroin, duration of heroin addition, duration of methadone treatment and the QTc intervals. The relations between gender and clinical variables such as SGOT, SGPT, γ-GT, HBsAg, and HCV Ab were assessed with the use of a Fisher's exact test. The QTc intervals were compared with the two-sample t-test for the normal and abnormal groups according to the classification from SGOT, SGPT, r-Gt, HBsAg, and HCV Ab. All statistical tests were two-sided, and a *p* value of less than 0.05 was considered to indicate statistical significance. Analyses were performed with the use of SAS software (version 9.1, SAS Institute).

To examine the association of the SNP, we used the $\chi 2$ test to compare the alteration of genotypes between patients and controls. The $\chi 2$ test evaluates the difference between the observed genotype frequency and the expected frequency under the null hypothesis of no association. However, when the expected frequency is small, the Fisher exact test is conducted instead. Bonferroni correction was applied for the multiple tests. Next, all detected SNPs were assessed for Hardy-Weinberg disequilibrium using the $\chi 2$ test. We conducted logistic regression analysis with a stepwise approach. The independent variables were values of SNP (homozygote, 2; heterozygote, 3; wild type, 1). The covariates of interactions between SNP were also included in the model. The final optimal model contains the statistically significant variables (SNP) that were selected by the stepwise procedure. These statistical analyses were performed using SPSS software (ver. 10.1; SPSS Science, Chicago, IL).

第三章　研究結果

第一節 基礎研究

首度發現內源性 CAPON 在心臟表達

我們使用 Western Blotting 的技術，從天筑鼠的左心室心肌尋找 CAPON protein 表達，心肌的 protein bands 和腦及肺組織 protein bands 作比對，我們也利用除了探求內源性的 capon 以外，我們也使用腺病毒載體（AdCAPON-GFP）將 CAPON 過度表達於 HEK293 細胞，Western Blot 的結果顯示心肌出現一個 60-Kda protein band，相當於內源性的 full-length CAPON，在 70-Kda protein band，可能是 CAPON 轉譯後改變或非特異性反應，值得注意的是，在心肌另外出現一條 30-Kda band，相當於 short-form CAPON，另外針對新分離之心室細胞作免疫及螢光染色也顯示 CAPON protein 在細胞質分佈並在細胞核與細胞膜周圍有加強的現象，在 CAPON 過度表達的心肌細胞也呈現免疫螢光增強現象，顯示腺病毒基因導入成功（AdCAPON-GFP）（圖 4）。

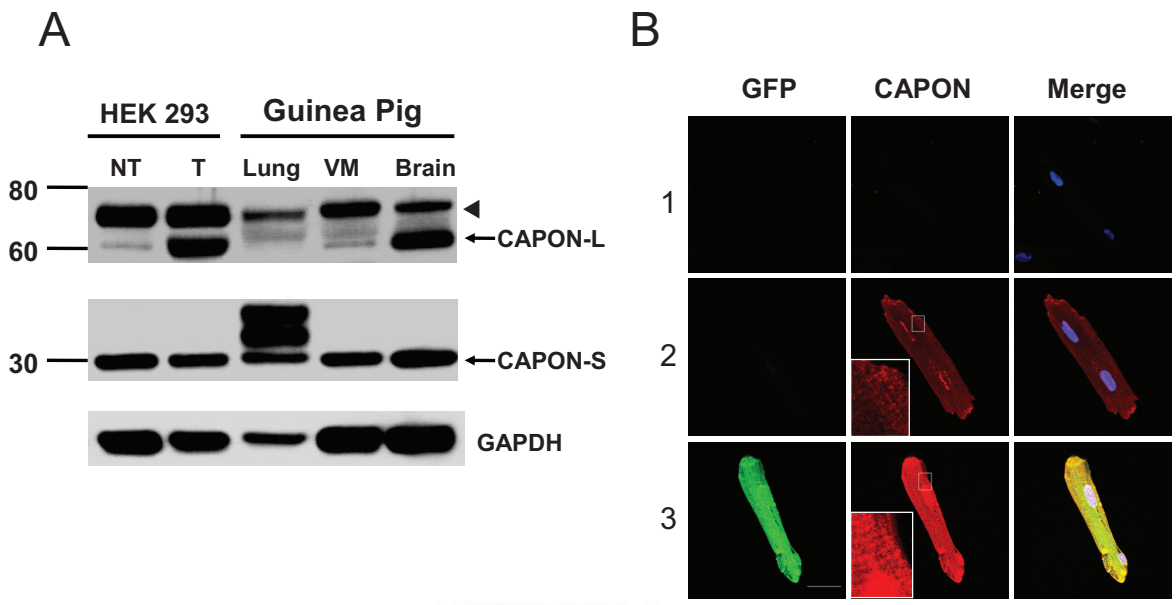

圖 4：CAPON 在心臟表達的證據。A：Western blot；B：免疫細胞染色。

腺病毒本身並不影響細胞電生理

為了證實腺病毒本身並不會改變細胞電生理，我們比較動作電位與鈣離子電流於 AdGFP 導入（transduction）與未導入（non-transduction）的心肌細胞，並發現這兩者並無顯著的差異（圖 5 A-B），在確定了腺病毒載體並不至導致細胞電生理的改變，我們才能夠進一步比較電生理特性於 AdCAPO-GFP 導入與未導入的心肌細胞。

CAPON 過度表達加速心室細胞動作電位

在 1-Hz 電刺激時，CAPON 過度表達的心肌細胞($n = 9$)其 APD_{10}、APD_{50}、APD_{75} 與 APD_{90} 分別降至 54.0 ± 7.2、198.8 ± 8.1、221.8

± 7.9 與 233.9 ± 7.7 ms，而對照之心肌細胞則為 96.6 ± 11.5、291.0 ± 16.4、316.1 ± 17.2 與 327.5 ± 17.9 ms (n＝13, P <0.05) (圖 5 C-E)。整體而言，CAPON 過度表達導致 APD_{90} 縮短 28.6%，接著我們進一步探討何種離子電流導致動作電位縮短。

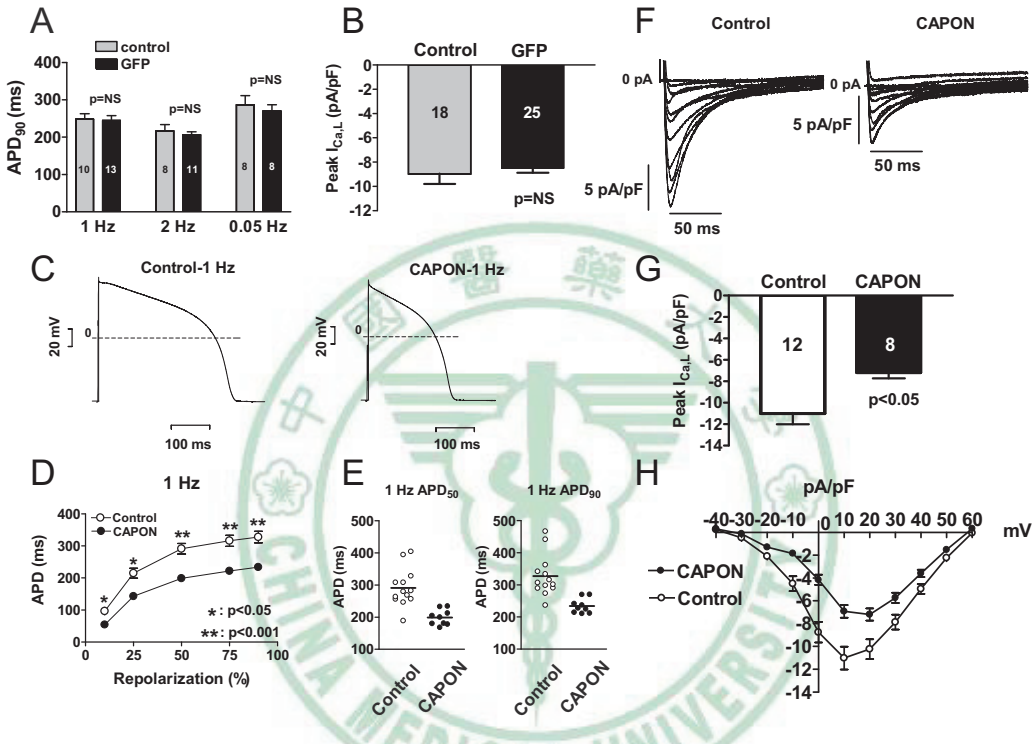

圖 5：CAPON 調控心肌細胞動作電位與鈣離子電流。

L-type 鈣離子電流

與對照之心肌細胞作比較，CAPON 過度表達的心肌細胞其密度明顯減少（-7.2 ± 0.5 pA/pF, at +20 mV, n＝8 vs. -11.0 ± 1.0 pA/pF, at +10 mV, n ＝12; P <0.05）（圖 5 F- G）整體而言，在 CAPON 過度表達的心肌細胞鈣離子密度約減少 35%，而 peak current density-voltage relationship (I-V curve) 分析顯示在 CAPON 過度表達的心肌細胞，其

膜電位從-30 mV 到+40 mV，其鈣離子電流都明顯的減小（圖 5 H），由於進入細胞的鈣離子電流減少，可導致 CAPON 過度表達之心肌細胞動作電位縮短。

鈉離子電流

鈉離子電流並未受到 CAPON 過度表達的影響（圖 6 A-B）。

向外整流之鉀離子電流 (Outward Rectifier Potassium Current)

在天竺鼠的心室肌肉細胞有兩種延遲向外整流之電流，即迅速活化性鉀離子電流（I_{Kr}）及緩慢性活化鉀電流（I_{Ks}），來負責終止動作電位的平原期，在探討 CAPON 過度表達在這兩種電流的影響，我們使用一種特異性的 I_{Ks} 阻斷劑 chromanol 293B 來分離 I_{Kr} 及 I_{Ks}，我們發現在 capon 過度表達的心肌細胞 I_{Kr} 的最大尾電流密度輕微增加（0.92 ± 0.07 pA/pF, $n = 10$ vs. 0.61 ± 0.08 pA/pF, $n = 7$; $P < 0.05$）（圖 6 C-D）這個結果顯示除了鈣離子電流減少外，I_{Kr} 電流的上升也有助於 CAPON 過度心肌細胞之動作電位的縮短。

向內整流之鉀離子電流 (Inward Rectifier Potassium Current，I_{K1})

向內整流之鉀離子電流 (I_{K1})並未受到 CAPON 的影響（圖 6 E）。

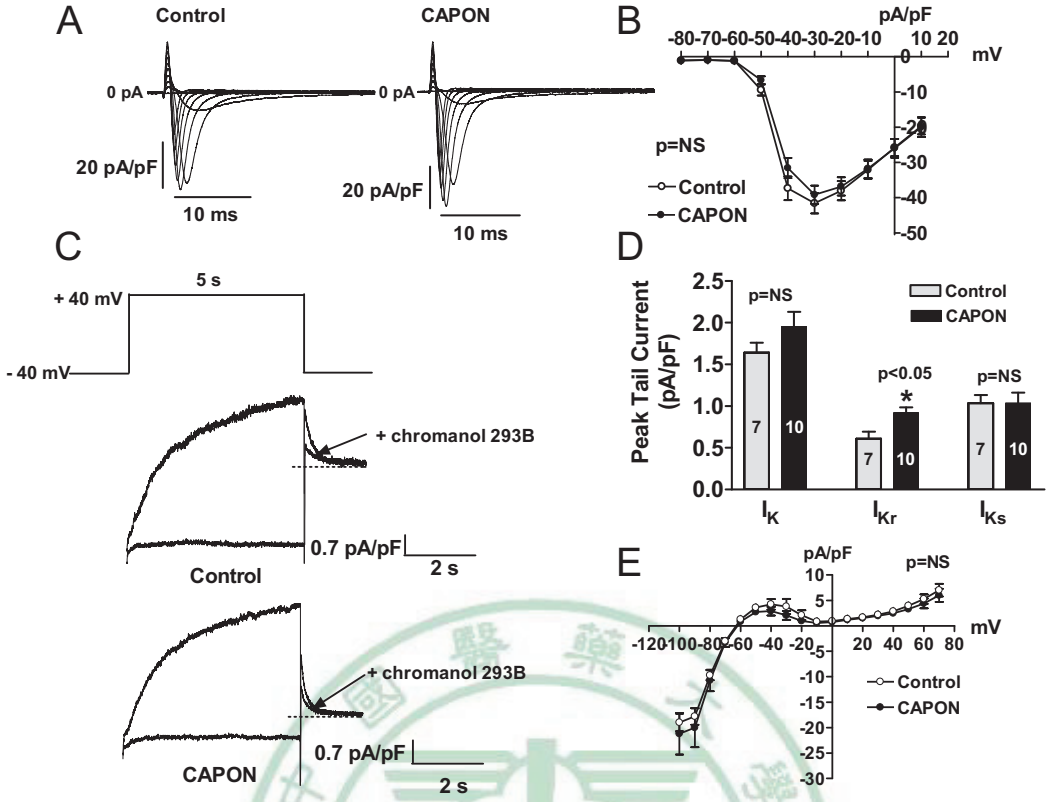

圖 6：CAPON 調控心肌細胞鉀離子電流。

CAPON 與 NOS1 蛋白-蛋白交互作用

在確定 full-length CAPON 與 short-form CAPON 確實在心臟表達，並且 CAPON 過度表達會透過減少鈣離子電流，及增強 I_{Kr} 電流使得心肌細胞之動作電位縮短後，我们接著探討 CAPON 過度表達後這些電生理現象的改變是否經由調控 NOS-NO 途徑，首先我們使用 CO-IP Western blot 來探討 CAPON-NOS 蛋白-蛋白交互作用，正常天竺鼠心肌細胞的均勻混合物，先和 anti-CAPON 或 anti-NOS1 結合的 Protein G complex 免疫反應後以 SDS/PAGE 分離，在分別用 CAPON NOS1 抗體去反應，我們發現 CAPON 只和 NOS1（圖 7 A-B）而不和

NOS3（圖 7 C-D）形成免疫沉澱，這個結果顯示 CAPON 和 NOS1 而不是和 NOS3 成為生理性複合體。

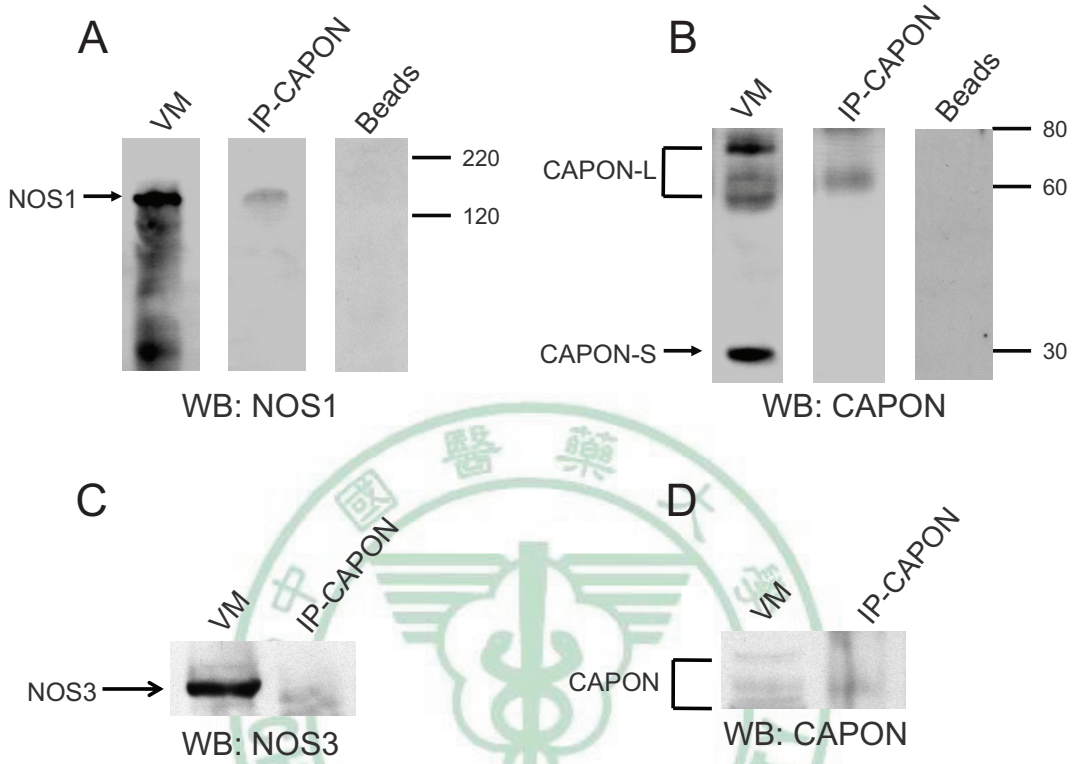

圖 7：CAPON 與 NOS1 在心臟呈現蛋白與蛋白之交互作用。

CAPON 過度表達 NOS1 穩定 NOS1

為了了解 CAPON 過度表達時 NOS1 蛋白如何改變，新分離的心室肌肉細胞接受 AdCAPON-GFP 或 AdGFP 之 in vitro 基因導入，或未接受任何基因導入，基因導入的效率在 AdGFP 組約為 100%（圖 8 A），在 AdCAPON-GFP 組約為 50%（圖 8 A），in vitro CAPON 基因導入可將 CAPON 蛋白的表達量增加為 1.9 倍（圖 8 B），在未作細胞培養之前，NOS1 蛋白量在 AdCAPON-GFP 導入與未接受基因導入的

心肌細胞是相近的（圖 8 C），可是在經過 40.3± 2.3 小時的細胞培養後，NOS1 蛋白在未接受基因導入與接受 AdGFP 導入的心肌細胞有明顯的下降，而在 AdCAPON-GFP 導入的心肌細胞則呈現穩定與增加，（2.78 ± 1.75% vs. 18.54 ± 5.99%, $P < 0.05$）（圖 8 D）。

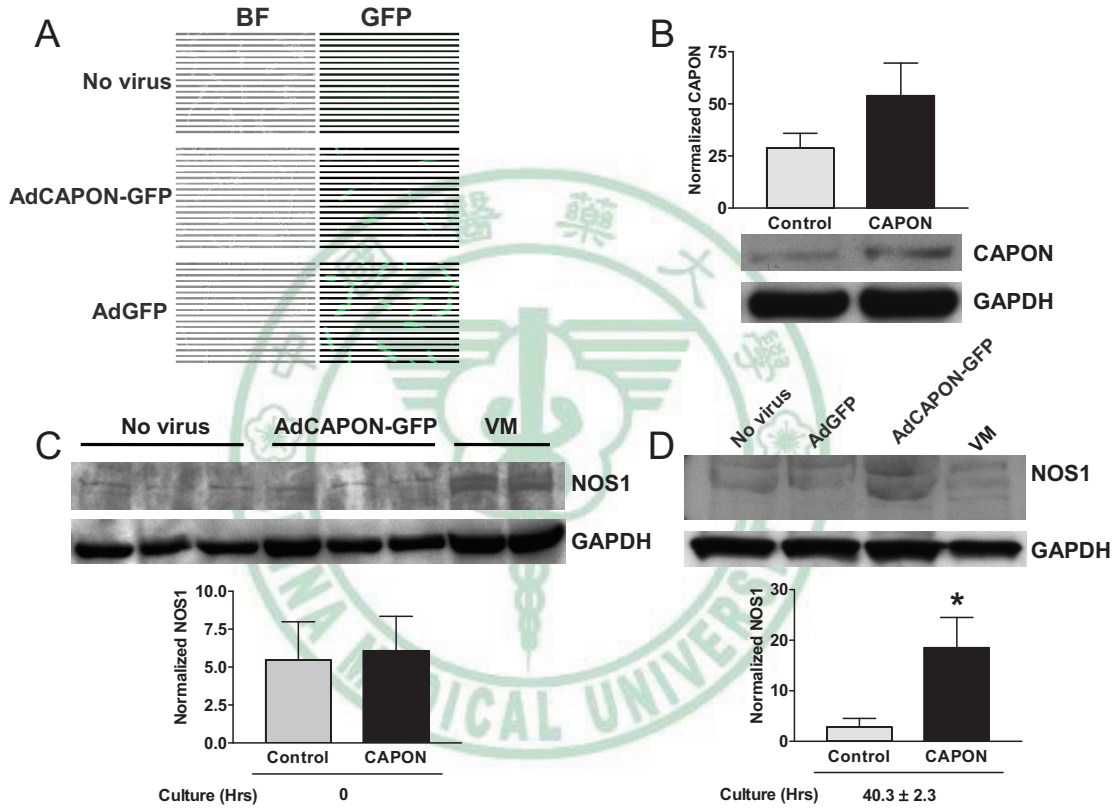

圖 8：在心肌細胞 CAPON 過度表達可穩定 NOS1 蛋白。

CAPON 過度表達心肌細胞可促使細胞內 NO 產量增加

在了解心肌細胞內 CAPON 與 NOS1 結合，可穩定 NOS1 後，我們進一步探討 CAPON 過度表達的心肌細胞其細胞內 NO 的產量是否改變，我們使用 DAR-4M AM 來測試存活細胞內之 NO 的含量，這些

心肌細胞是在 *in vivo* CAPON 基因導入 3-5 天後分離所得，DAR-4M AM 的螢光特異性先經過加入 L-NAME 後螢光減弱，與加入 sodium nitroprusside 螢光增強而證實（圖 9 A），我們接著在 baseline 時與加入 L-arginine 後，比較細胞內的 NO 產量並發現當心肌細胞加了 L-arginine 之後，CAPON 過度表達的心肌細胞螢光強度大於對照組的心肌細胞，（1420.9 ± 28.1 a.u. n＝43 vs. 1329.0 ± 19.1 a.u., n＝166, P <0.05）（圖 9 B-D）。

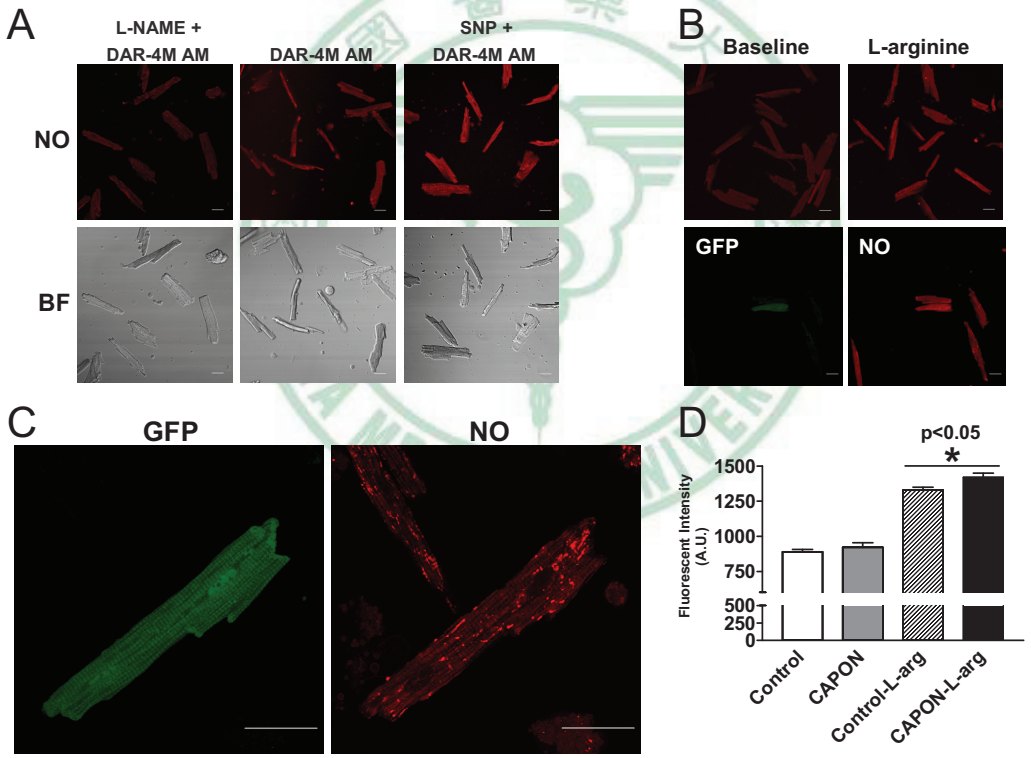

圖 9：在心臟 CAPON 過度表達可提升心肌細胞的 NO 產量。

L-NAME 恢復 CAPON 過度表達引起的動作電位縮短與鈣離子電流減少

在 3-5 天後，將接受 *in vivo* CAPON 基因導入之心肌細胞分離

後，加與不加 1mM L-NAME 後，在分別測試其動作電位與鈣離子電流的影響，我們發現於 CAPON 過度表達的心肌細胞加了 L-NAME 後，原本縮短的 APD_{90} 恢復至與對照組細胞相近的 APD_{90}（1 Hz, 348.3 ± 47.8ms, n＝7 vs. 221.6 ± 19.9 ms, n＝6, P <0.05）（圖 10 A-B），而原本減少的鈣離子電流也恢復至對照組細胞的水準（-6.2 ± 0.6 pA/pF, n ＝14 vs. -4.8 ± 0.3 pA/pF, n ＝14; P <0.05）（圖 10 C-E）。

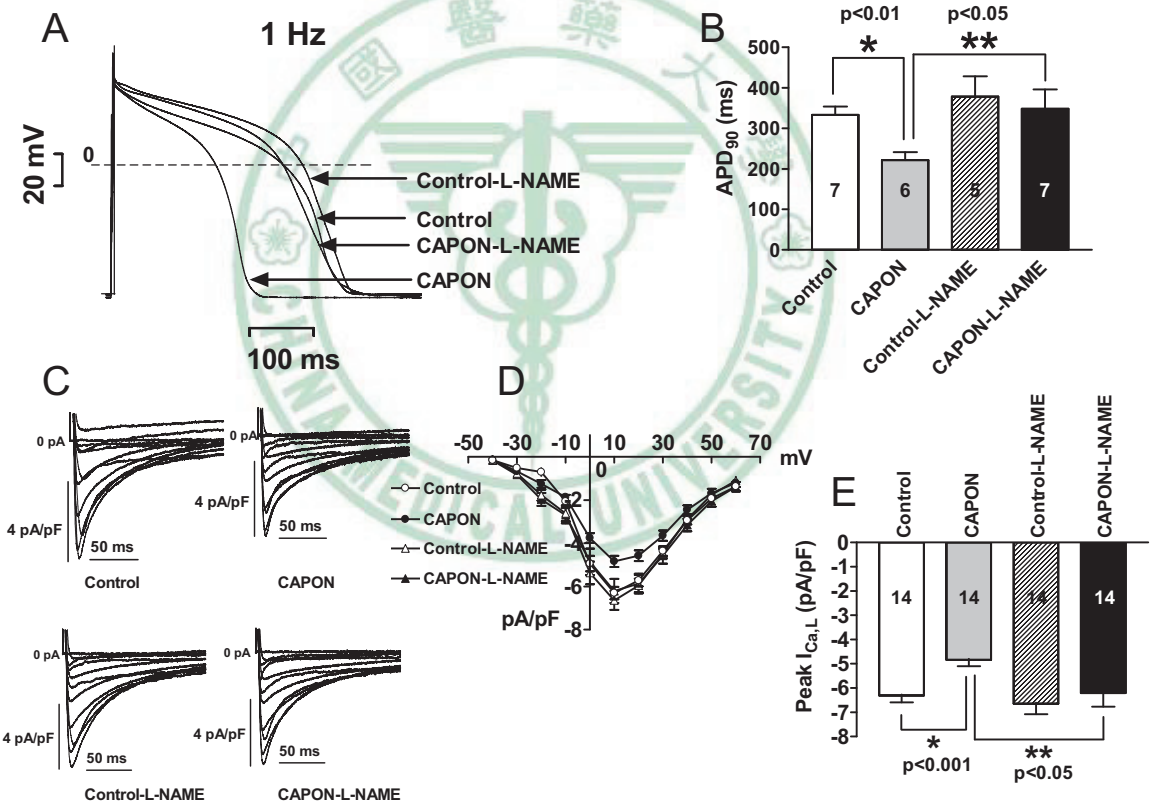

圖 10：L-NAME 可拮抗因 CAPON 過度表達引起心肌細胞動作電位縮短與鈣離子電流變小。

第二節 臨床研究

Methadone 劑量和心電圖 QTc－Cross Section 分析

在這一部份分析裡面共有 203 位海洛因成癮正在接受 Methadone 治療的病人，他們的基本資料如表 2 所示，男性有 164 人，女性有 39 人，年紀分別為男性 38.9 ± 7.1 歲，女性 35.2 ± 6.7 歲，接受 Methadone 治療的劑量，男性 48.6 ± 25.6 mg，女性 44.6 ± 25.7 mg。

表 2：cross-section 病人組的基本資料。

Variables	All（N=203）	Male（N=164）	Female（N=39）	p-value
	mean±SD	mean±SD	mean±SD	
Age（year）	38.2 ± 7.2	38.9 ± 7.1	35.2 ± 6.7	0.0029[b]
First use of heroin（age, years）	26 ± 7.2	26 ± 7.4	26 ± 6.7	0.9962[b]
QTc（ms）	430.1 ± 22.0	429.1 ± 21.7	434.5 ± 23.0	0.1621[b]
Normal, N（%）	116（57.1）	86（52.4）	30（76.9）	0.0055[c]
Abnormal[a],N（%）	87（42.9）	78（47.6）	9（23.1）	
Methadone dose（mg）	47.8 ± 25.6	48.6 ± 25.6	44.6 ± 25.7	0.3819[b]
Heroin addiction（years）	12.2 ± 6.1	12.9 ± 6.0	9.2 ± 6.0	0.0005[b]
MMT（days）	246 ± 191.3	254.3 ± 194.6	211 ± 174.8	0.2045[b]
a： Female and QTc＞450 ms；male and QTc＞430 ms				
b： Two sample t-test				
c： Chi-square test				

在男性 Methadone 劑量和心電圖的 QTC 呈現顯著的正相關（圖 11），而在女性病人則沒有相關性（圖 12），在男性病人，單變相與多變相分析都顯示 Methadone 劑量是和 QTc 延長最顯著相關的因素（表 3），在女性病人，不管用單變相與多變相分析都顯示 Methadone

劑量是和 QTc 延長沒有顯著的相關性（表 4）。

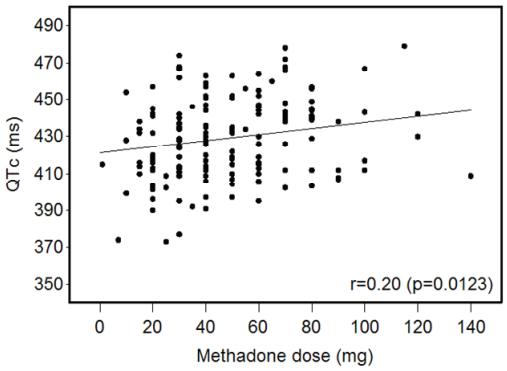

Male: Dose-dependent Correlation
mean methadone dose 48.6 mg

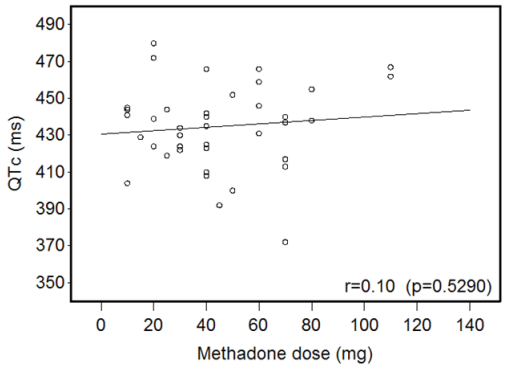

Female: Dose-dependent Correlation
mean methadone dose 44.6 mg

圖 11（左）：methadone 劑量與 QTc 在男性呈現正相關。

圖 12（右）：methadone 劑量與 QTc 在女性不呈正相關性。

表 3：cross-section 分析，男性病人的 methadone 劑量與 QTc 呈正相關性。

Positive Dose-dependent Association Between Methadone and QTc in Male Subjects

Male（N=164）	Univariate analysis		Univariate analysis	
	Beta	p-value	Beta	p-value
Methadone dose（mg）	0.165	0.012	0.187	0.005
Age（years）	0.373	0.119	0.555	0.033
First use of heroin（age, years）	0.392	0.090		
Heroin addiction（years）	-0.076	0.793	-0.327	0.282
MMT（days）	0.006	0.503	0.004	0.667

表 4：cross-section 分析，女性病人的 methadone 劑量與 QTc 不呈正相關性。

Negative Dose-dependent Association Between Methadone and QTc in Female Subjects

Female（N=39）	Univariate analysis		Univariate analysis	
	Beta	p-value	Beta	p-value
Methadone dose（mg）	0.093	0.529	0.191	0.278
Age（years）	0.413	0.467	0.935	0.211
First use of heroin（age, years）	0.492	0.384		
Heroin addiction（years）	-0.099	0.875	-0.545	0.472
MMT（days）	-0.007	0.760	0.004	0.853

Methadone 劑量和心電圖 QTc－Longitudinal 分析

在這一部份分析裡面共有 55 位海洛因成癮正在接受 Methadone 治療的病人，他們的基本資料如表 5 所示，男性有 46 人，女性有 9 人，年紀分別為男性 37.5 ± 7.0 歲，女性 33.1 ± 5.1 歲，男性在接受 Methadone 治療前的 QTc 是 427.0 ± 23.4 ms，治療一個月後（55.3 ± 24.0 mg），QTc 顯著延長為 431.0 ± 21.3 ms （$P=0.026$）（圖 13），而女性在接受 Methadone 治療前的 QTc 是 437.6 ± 32.9 ms，治療一個月後（52.5 ± 23.1 mg），QTc 並無顯著變化為 420.5 ± 22.4 ms（$P=0.297$）（圖 14）。

表 5：Longitudinal 分析組病人的資料。

Baseline Characteristics of Study Subjects

Table 1. When time = 0

Variables	All（N=55）	Male（N=46）	Female（n=9）	p-value[a]
Age（years）	36.8 ± 6.9	37.5 ± 7.0	33.2 ± 5.1	0.096
First use of heroin（age, years）	25 ± 7.1	24.8 ± 7.3	26.4 ± 6.2	0.32
Heroin addiction（years）	11.7 ± 6.6	12.7 ± 6.5	6.8 ± 4.7	0.007
MMT（days）	25 ± 94.9	29.9 ± 103.3	23.2 ± 102.3	0.316

a：Wilcoxon rank sum test

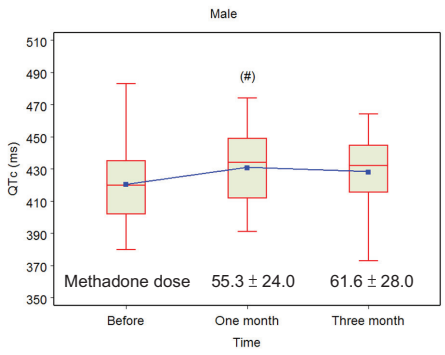

Significant QTc Prolongation After Methadone Treatment in Male

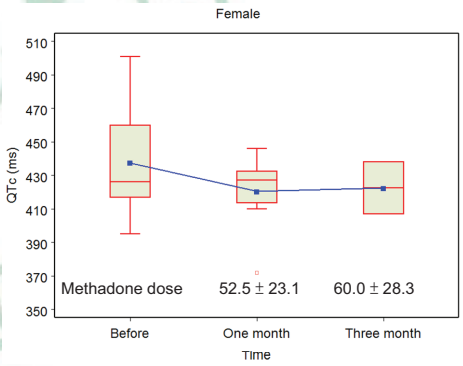

Insignificant QTc Change After Methadone Treatment in Female

圖 13（左）：Longitudinal 分析，男性病人在 methadone 治療後 QTc 顯著延長。

圖 14（右）：Longitudinal 分析，女性病人在 methadone 治療後 QTc 沒有顯著延長。

CAPON 基因變異、Methadone 劑量與心電圖 QTc

我們初步基因鑑定 24 個 CAPON SNPs，包括 rs10494366、rs10918594、rs1415263 等，來看帶有 CAPON SNPs 者是否進一步加強 Methadone 對 QTC 的影響，我們以 111 位海洛英成癮預備接受 methadone 治療的 101 位男性病人做分析，在還沒有接受 methadone 治療前，以 rs10918594CC 為 reference (frequency 為 52.81%)，其 QTc 為 421.9± 23.8 ms，帶有 rs10918594CG 者(frequency 為 16.85%)，其 QTc 延長 7.46 ms（p＝0.284），而帶有 rs10918594GG 者(frequency 為 30.34%)，其 QTc 進一步延長 11.60 ms（p＝0.040），顯示 rs10918594 基因變異與 QTc 延長，具有 dose-dependent effect，而另一著名 SNP、rs10494366 在歐美族群和 QTc 延長具有非常顯著相關性的基因變異，在目前我們研究族群，則不具有和 QTc 延長的相關性。在服用 methadone（48.6 ± 10.3 mg） 36 ± 10 天後，帶有 rs10918594CG 者，其 QTc 的變化不明顯（-0.88 ms，p＝0.930），而帶有 rs10918594GG 者，其 QTc 進一步延長為 15.41 ms（p＝0.0486），此結果顯示 CAPON 基因變異（rs10918594）加上 methadone 使用，對 QTc 延長具有加成作用（表 6）。

表 6：CAPON 基因變異、methadone 和 QTc 的相關性。

CAPON gene variants, methadone and QTc

Variables	Before Methadone				After Methadone			
	n	QTc	95% CI	p	n	QTc	95% CI	p
rs1964052_CC	63		reference		40			
rs1964052_CT	26	7.6	(-3.2 , 18.3)	NS	14	-0.4	(-15.9 , 15.1)	NS
rs1964052-TT	1	20.2	(-26.3 , 66.8)	NS	1	8.5	(-42.2 , 59.2)	NS
rs10918594_CC	47		reference		34			
rs10918594_CG	15	7.5	(-6.3 , 21.2)	0.284	7	-0.9	(-20.8 , 19.0)	NS
rs10918594_GG	27	11.6	(0.6 , 22.6)	0.040	14	15.4	(0.1 , 30.7)	0.0486
rs10494366_GG	48		reference		26			
rs10494366_GT	35	-6.9	(-17.2 , 3.4)	NS	24	-6.0	(-20.1 , 8.2)	NS
rs10494366_TT	7	-4.9	(-23.7 , 13.8)	NS	5	-4.0	(-28.4 , 20.5)	NS
rs348624_CC	61		reference		41			
rs348624_CT	22	8.4	(-3.4 , 20.2)	NS	13	-0.7	(-16.4 , 15.0)	NS
rs348624_TT	1	20.7	(-27.2 , 68.5)	NS	1	9.2	(-40.6 , 58.9)	NS

第四章　討論

第一節 基礎研究

我們首度證實 CAPON 這一個在腦神經組織相當重要的 NOS1 的 adaptor/regulator 蛋白也在心臟表達並且和 NOS1 交互作用，當 CAPON 過度表達時會活化 NOS1-NO 訊息傳遞路徑，使得鈣離子電流減小，Ikr 電流增加，導致動作電位縮短。

內源性 CAPON 於心臟表達

自從 1998 年 CAPON 在大鼠腦神經被發現以後，Xu. et al. 進一步證實 CAPON 蛋白有兩種 isooforms：full-length CAPON 與 short-form C terminus CAPON，full-length CAPON 含有 10 個 exons，並形成 PTB-與 PDZ-binding dormains，我們也首度證實這兩種 CAPON isoforms 都在心臟表達，細胞免疫螢光顯示 CAPON 蛋白分部於細胞質，並且在細胞核周圍與細胞膜有增強現象。

CAPON 過度表達活化 NOS1-NO 路徑

為了證實 CAPON 過度表達能活化 NOS1-NO 路徑，並且造成細胞電生理的改變，我們使用 Co-IP Western blot 證實 CAPON NOS1 具有蛋白-蛋白交互作用，這種交互作用也經由使用共軛焦顯微鏡檢細胞免疫螢光染色，顯示 CAPON 與 NOS1 呈現細胞內 colocalization 的

現象（圖 15），有趣的是只有 full-length CAPON 才與 NOS1 有交互作用，這和過去在腦神細胞觀察到的現象一致，接著我們使用體外基因導入與細胞培養的方式，證實 CAPON 過度表達可以穩定 NOS1，此爲 CAPON 與 NOS1 在心臟之交互作用提供更為直接之證據，最後我們使用 DAR-4M AM 來直接測試活體心肌細胞內 NO 的產量，並發現 CAPON 過度表達細胞內 NO 產量上升，雖然比起對照組心肌細胞 CAPON 過度表達只是造成少許 NO 產量增加（7 %），但由於 NO 的生理作用，與負責產生 NO 的 NOS 所在的位置息息相關，而 CAPON 很可能把 NOS 帶到特定的標的蛋白，使 NO 發揮特定的作用，另外由於 CAPON 能夠和其他蛋白競爭 PDZ-binding，CAPON 也有可能經由此一機轉行使其生理作用。

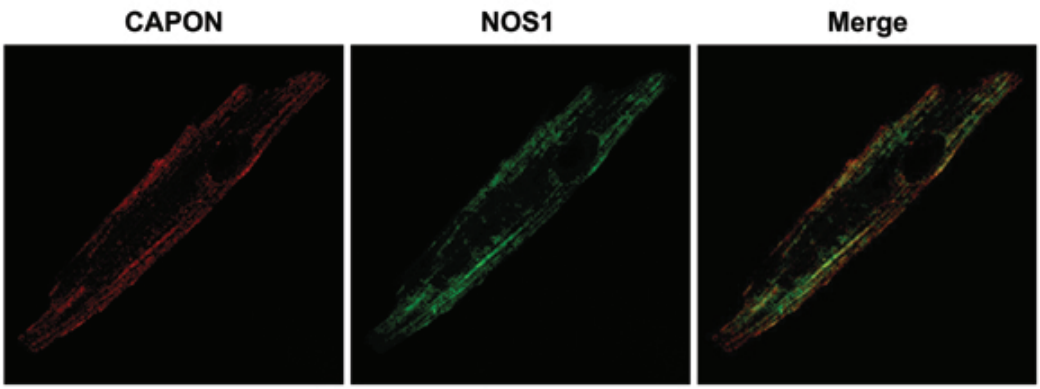

圖 15：共軛焦顯微鏡檢細胞免疫螢光染色，顯示 CAPON 與 NOS1 呈現細胞內 colocalization 的現象。

CAPON 過度表達透過抑制鈣離子電流與提升 Ikr 來縮短動作電位

由於天筑鼠的心肌細胞缺少 I_{to} 電流，根據本實驗結果，鈣離子電流減少 35%，I_{kr} 電流增加 50%，已足以解釋動作電位縮短 30%在 CAPON 過度表達的心肌細胞。

L-NAME 可恢復 CAPON 過度表達所引起的電生理變化

我們分別加 L-NAME 過度達的心肌細胞與對照組的心肌細胞，結果發現 L-NAME 於 CAPON 過度表達的心肌細胞於延長 APD_{90}（57% vs. 13%）與提升鈣離子電流（29% vs.5%）的強度均較對照組心肌細胞更為顯著，如此可排除 L-NAME 的 background effect，並證實 CAPON 過度表達造成的電生理改變確實是透過 NOS1-NO 途徑所致，至於 NO 如何經由抑制鈣離子電流及提升 I_{ks} 電流來縮短動作電位，過去研究顯示 NO 可以透過 cGMP-dependent 與 cGMP-independent 的途徑來抑制細胞膜鈣離子電流，相同的 NO 也可能透過相同的機制，影響細胞膜 I_{kr} 電流，根據 Burkard 的研究顯示在 NOS1 過度表達的基因轉殖鼠，在 NOS1 過度表達的心肌細胞其鈣離子電流減少 39%，這是因為 NOS1 被帶到細胞膜並和 L-type 鈣離子通道蛋白交互作用所致，因此我們很有理由相信當 CAPON 過度表達時，將 NOS1 帶到細胞膜並與細胞膜的離子蛋白交互作用，使得鈣離子電流減少與 I_{kr} 電流增加，而導致動作電位縮短。

第二節　臨床研究

1）Methadone 劑量與 QTc 關係

我們發現不管從 cross-section 或 longitudinal 分析，男性病人的 QTc 和 methadone 劑量都呈現很顯著的正相關性，而女性病人則無此現象，有趣的是目前文獻報告 methadone 劑量和 QTc 延長呈現正相關性，其所使用的平均數或中位數 methadone 劑量都在 100 mg 以上，而在本研究中男性病人使用 methadone 的平均劑量只有 48.6 mg，這是第一篇的研究顯示低劑量的 methadone 仍然與 QTc 的延長有正相關性，此外，methadone 劑量與 QTc 延長是否存在性別的差異，Fanoe 在他們的 cross-section 研究中指出，男性病人的相關係數 correlation coefficient 為 0.28，而女性只有 0.12，似乎透露出接受 methadone 治療的男性病人較容易出現 QTc 延長，而我們的研究是首度使用 cross-section 及 longitudinal 的分析，指出男性比女性在接受 methadone 治療後更易出現 QTc 延長，這和傳統上女性病人較容易引起藥物性 QTc 延長的認知有所不同。

2）CAPON 基因變異、methadone 與 QTc 關係

我們根據文獻報告篩選 24 個可能跟 QTc 延長有關的 CAPON 基因變異，初步發現 rs10918594GG 的基因變異（wild type 為 rs10918594CC），與 QTc 延長具有顯著的相關性，這些帶有

rs10918594GG 的基因變異者，在接受 methadone 治療一個月後，QTc 進一步的延長，具有加成作用，這是第一次在歐美以外的族群發現 CAPON 變異與 QTc 延長的相關性，在臨床意義上，若帶有 CAPON 基因變異再加上使用 QTc 延長藥物時（例如 methadone），就必須特別注意 QTc 是否過度延長，導致致命性心律不整。

第三節　研究限制

目前研究限於細胞膜上的電流，並未擴及研究細胞內的鈣離子訊號（caclciun transients）與興奮－收縮交替作用（excitation-contraction copuling），因為過去研究顯示 NOS1-NO 也和調節心臟收縮有關，使得這一部分的研究顯得相當重要，再者，由於 CAPON 能夠和其他蛋白競爭 PDZ-binding，CAPON 也有可能經由此一機轉行使其生理作用（NO-independent）而不單由 NO-dependent 的機轉。最後本研究未能檢視動物在接受 CAPON 基因過度表達後之 ECG phenotype，這是由於受限於 gene transfer 的效率只達 1-10%，因此將來可能需要使用 CAPON 基因轉殖或剔除的動物模式的研究來回答以上的問題。

在臨床上的限制為：1）未能偵測 methadone 血中濃度，僅以口服 methadone 劑量高低代表體內 methadone 濃度高低，忽視了 methadone 吸收與代謝的因素；2）CAPON 基因鑑定個案數不夠多，

可能需更大型的研究來驗證結果。

第五章　結論

經由基礎研究我們發現CAPON蛋白在心臟表達並與NOS1交互作用而調節心臟生理機能，CAPON過度表達可以穩定NOS1並且活化NOS1-NO訊息傳遞路徑，使得鈣離子電流減小與Ikr電流增加導致動作電位縮短，此一基礎研究提供臨床上發現之CAPON基因變異和心電圖 QTc 相關性的理論基礎，更進一步而言，我們認為在noncoding region的基因變異可能改變了CAPON在心臟的表達量，進而影響心臟的在極化與心電圖的QT interval。

在臨床研究方面，我們首度發現低劑量的methadone與QTc延長有顯著的相關性。而這種相關性在男性更為顯著，在女性則不顯著。此一性別敏感性差異，和我們過去所認知的藥物引起的 QTc 延長通常發生在女性的論點大異其趣，值得進一步研究。另外，在基因研究方面，我們也首度發現CAPON SNP rs10918594除了在西方族群會與QTc延長相關外，在亞洲族群也存在這個相關性，需進一步在更大型的研究證實。

參考文獻

1. Arking, D. E., Pfeufer, A., Post, W., Kao, W. H., Newton-Cheh, C., Ikeda, M., West, K., Kashuk, C., Akyol, M., Perz, S., Jalilzadeh, S., Illig, T., Gieger, C., Guo, C. Y., Larson, M. G., Wichmann, H. E., Marban, E., O'Donnell, C. J., Hirschhorn, J. N., Kaab, S., Spooner, P. M., Meitinger, T. & Chakravarti, A. (2006) *Nat Genet* **38,** 644-51.
2. Post, W., Shen, H., Damcott, C., Arking, D. E., Kao, W. H. L., Sack, P. A., Ryan, K. A., Chakravarti, A., Mitchell, B. D. & Shuldiner, A. R. (2007) *Human Heredity* **64,** 214.
3. Aarnoudse, A.-J. L. H. J., Newton-Cheh, C., de Bakker, P. I. W., Straus, S. M. J. M., Kors, J. A., Hofman, A., Uitterlinden, A. G., Witteman, J. C. M. & Stricker, B. H. C. (2007) *Circulation* **116,** 10-16.
4. Jaffrey, S. R., Snowman, A. M., Eliasson, M. J., Cohen, N. A. & Snyder, S. H. (1998) *Neuron* **20,** 115-24.
5. Fang, M., Jaffrey, S. R., Sawa, A., Ye, K., Luo, X. & Snyder, S. H. (2000) *Neuron* **28,** 183-93.
6. Jaffrey, S. R., Benfenati, F., Snowman, A. M., Czernik, A. J. & Snyder, S. H. (2002) *Proc Natl Acad Sci U S A* **99,** 3199-204.
7. Hare, J. M. & Stamler, J. S. (2005) *J. Clin. Invest.* **115,** 509-517.

8. Xu, K. Y., Kuppusamy, S. P., Wang, J. Q., Li, H., Cui, H., Dawson, T. M., Huang, P. L., Burnett, A. L., Kuppusamy, P. & Becker, L. C. (2003) *J Biol Chem* **278,** 41798-803.

9. Oceandy, D., Cartwright, E. J., Emerson, M., Prehar, S., Baudoin, F. M., Zi, M., Alatwi, N., Schuh, K., Williams, J. C., Armesilla, A. L. & Neyses, L. (2007) *Circulation* **115,** 483-492.

10. Barouch, L. A., Harrison, R. W., Skaf, M. W., Rosas, G. O., Cappola, T. P., Kobeissi, Z. A., Hobai, I. A., Lemmon, C. A., Burnett, A. L., O'Rourke, B., Rodriguez, E. R., Huang, P. L., Lima, J. A. C., Berkowitz, D. E. & Hare, J. M. (2002) *Nature* **416,** 337.

11. Xu, K. Y., Huso, D. L., Dawson, T. M., Bredt, D. S. & Becker, L. C. (1999) *Proc Natl Acad Sci U S A* **96,** 657-62.

12. Burkard, N., Rokita, A. G., Kaufmann, S. G., Hallhuber, M., Wu, R., Hu, K., Hofmann, U., Bonz, A., Frantz, S., Cartwright, E. J., Neyses, L., Maier, L. S., Maier, S. K. G., Renne, T., Schuh, K. & Ritter, O. (2007) *Circ Res* **100,** e32-44.

13. Xu, B., Wratten, N., Charych, E. I., Buyske, S., Firestein, B. L. & Brzustowicz, L. M. (2005) *PLoS Med* **2,** e263.

14. Sanguinetti, M. C. & Jurkiewicz, N. K. (1990) *J. Gen. Physiol.* **96,**

195-215.

15. Bosch, R. F., Gaspo, R., Busch, A. E., Lang, H. J., Li, G.-R. & Nattel, S. (1998) *Cardiovascular Research* **38,** 441.

16. Inoue, M. & Imanaga, I. (1993) *Am J Physiol* **264,** C1434-8.

17. Bai, C. X., Takahashi, K., Masumiya, H., Sawanobori, T. & Furukawa, T. (2004) *Br J Pharmacol* **142,** 567-75.

18. Bai, C. X., Namekata, I., Kurokawa, J., Tanaka, H., Shigenobu, K. & Furukawa, T. (2005) *Circ Res* **96,** 64-72.

19. Campbell, D. L., Stamler, J. S. & Strauss, H. C. (1996) *J. Gen. Physiol.* **108,** 277-293.

20. Furukawa, T., Bai, C.-X., Kaihara, A., Ozaki, E., Kawano, T., Nakaya, Y., Awais, M., Sato, M., Umezawa, Y. & Kurokawa, J. (2006) *Mol Pharmacol* **70,** 1916-1924.

21. Han, N.-L. R., Ye, J.-S., Yu, A. C. H. & Sheu, F.-S. (2006) *J Neurophysiol* **95,** 2167-2178.

22. Sears, C. E., Bryant, S. M., Ashley, E. A., Lygate, C. A., Rakovic, S., Wallis, H. L., Neubauer, S., Terrar, D. A. & Casadei, B. (2003) *Circ Res* **92,** e52-9.

23. Manfredi PL, Borsook D, Chandler SW, Payne R. Intravenous

methadone for cancer pain unrelieved by morphine and hydromorphone: clinical observations. *Pain* 1997;70:99.

24. Lisa AM. The efficacy of methadone maintenance interventions in reducing illicit opiate use, HIV risk behavior and criminality: a meta-analysis. *Addiction* 1998;93:515-532.

25. Ricardo AC, Ryuichi S, Peter H, David L, Ysmael Y, Yukako S, Paul S, Stanley RY, Jeanne AL, Lauren S, Robert GS, Russell KP. Measurement of QTc in Patients Receiving Chronic Methadone Therapy. *Journal of pain and symptom management* 2005;29:385.

26. Joseph HS, Sharon. Langrod, John. Methadone maintenance treatment (MMT): a review of historical and clicnical issues. *Mt Sinai J Med* 2000;67:347-364.

27. Matthew H, Peter M, John H, Allan B, Chris W, Jon W, Gerry S, Paul E. Trends in drug overdose deaths in England and Wales 1993–98: methadone does not kill more people than heroin. *Addiction* 2003;98:419-425.

28. Ballesteros MF, Budnitz DS, Sanford CP, Gilchrist J, Agyekum GA, Butts J. Increase in Deaths Due to Methadone in North Carolina. *JAMA* 2003;290:40-.

29. Krantz MJ, Lewkowiez L, Hays H, Woodroffe MA, Robertson AD, Mehler PS. Torsade de Pointes Associated with Very-High-Dose Methadone. *Ann Intern Med* 2002;137:501-504.

30. Paul WW, Douglas K, Leslie K. High dose methadone and ventricular arrhythmias: a report of three cases. *Pain* 2003;103:321.

31. Kornick CA, Kilborn MJ, Santiago-Palma J, Schulman G, Thaler G, Keefe DL, Katchman AN, Pezzullo DL, Ebert SN, Woosley RL, Payne R, Manfredi PL. QTc interval prolongation associated with intravenous methadone. *Pain* 2003;105:499-506.

32. Katchman AN, McGroary KA, Kilborn MJ, Kornick CA, Manfredi PL, Woosley RL, Ebert SN. Influence of Opioid Agonists on Cardiac Human Ether-a-go-go-related Gene K+ Currents. *J Pharmacol Exp Ther* 2002;303:688-694.

33. Mattick RP, Kimber J, Breen C, Davoli M. Buprenorphine maintenance versus placebo or methadone maintenance for opioid dependence. *Cochrane Database of Systemic Reviews* 2008:CD002207.

34. Ehret GB, Voide C, Gex-Fabry M, Chabert J, Shah D, Broers B, Piguet V, Musset T, Gaspoz J-M, Perrier A, Dayer P, Desmeules JA.

Drug-Induced Long QT Syndrome in Injection Drug Users Receiving Methadone: High Frequency in Hospitalized Patients and Risk Factors. *Arch Intern Med* 2006;166:1280-1287.

35. Fanoe S, Hvidt C, Ege P, Jensen GB. Syncope and QT prolongation among patients treated with methadone for heroin dependence in the city of Copenhagen. *Heart* 2007;93:1051-1055.

36. Peles E, Bodner G, Kreek MJ, Rados V, Adelson M. Corrected-QT intervals as related to methadone dose and serum level in methadone maintenance treatment (MMT) patientsa cross-sectional study. *Addiction* 2007;102:289.

37. Katinka A, Thomas C, Michael G, Viggo H, Helge W. Prevalence and clinical relevance of corrected QT interval prolongation during methadone and buprenorphine treatment: a mortality assessment study. *Addiction* 2009;104:993-999.

38. Walker PW, Klein D, Kasza L. High dose methadone and ventricular arrhythmias: a report of three cases. *Pain* 2003;103:321.

39. Ellen CP, Raymond LW. QT prolongation and torsades de pointes among methadone users: reports to the FDA spontaneous reporting system. *Pharmacoepidemiology and Drug Safety* 2005;14:747-753.

40. Malhotra BK, Glue P, Sweeney K, Anziano R, Mancuso J, Wicker P. Thorough QT Study with Recommended and Supratherapeutic Doses of Tolterodine. *Clin Pharmacol Ther* 2007;81:377-385.

41. Reinig MG, Engel TR. The Shortage of Short QT Intervals*. *Chest* 2007;132:246-249.

42. Rautaharju PM, Kooperberg C, Larson JC, LaCroix A. Electrocardiographic Predictors of Incident Congestive Heart Failure and All-Cause Mortality in Postmenopausal Women: The Women's Health Initiative. *Circulation* 2006;113:481-489.

43. Carnethon MR, Prineas RJ, Temprosa M, Zhang Z-M, Uwaifo G, Molitch ME. The Association Among Autonomic Nervous System Function, Incident Diabetes, and Intervention Arm in the Diabetes Prevention Program. *Diabetes Care* 2006;29:914-919.

44. Lehtinen AB, Newton-Cheh C, Ziegler JT, Langefeld CD, Freedman BI, Daniel KR, Herrington DM, Bowden DW. Association of NOS1AP Genetic Variants With QT Interval Duration in Families From the Diabetes Heart Study. *Diabetes* 2008;57:1108-1114.

45. Tyl B, Kabbaj M, Fassi B, De Jode P, Wheeler W. Comparison of Semiautomated and Fully Automated Methods for QT Measurement

During a Thorough QT/QTc Study: Variability and Sample Size Considerations. *J Clin Pharmacol* 2009;49:905-915.

46. Fosser C, Duczynski G, Agin M, Wicker P, Darpo B. Comparison of Manual and Automated Measurements of the QT Interval in Healthy Volunteers: An Analysis of Five Thorough QT Studies. *Clin Pharmacol Ther* 2009:advance online publication 1 April 2009.

47. Bazett HC. An analysis of the time-relations of electrocardiograms. *Heart* 1920;7:353-370.

48. Yap YG, Camm AJ. Drug induced QT prolongation and torsades de pointes. *Heart* 2003;89:1363-1372.

附　錄

1. Kuan-Cheng Chang, Andreas S. Barth, Eddy Kizana, Yuji Kashiwakura, Tetsuo Sasano, Yiqiang Zhang, Hee Cheol Cho, Ting Liu, Eduardo Marbán, CAPON, a Nitric Oxide Synthase Regulator Associated with QT Interval Variation in Humans, Modulates Cardiac Repolarization in Ventricular Myocytes. Circulation, 2006;114(18):II-167 (Supplement)
2. Kuan-Cheng Chang, Andreas S. Barth, Tetsuo Sasano, Yiqiang Zhang, Junichiro Miake, Eduardo Marbán, *CAPON* Interacts With Neuronal Nitric Oxide Synthase To Modulate L-type Calcium Current And Action Potential Duration In Ventricular Cardiomyocytes. Circulation, Oct 2007;116:II-11-12 (Supplement)
3. Kuan-Cheng Chang, Andreas S. Barth, Tetsuo Sasano, Eddy Kizana, Yuji Kashiwakura, Yiqiang Zhang, D. Brian Foster, and Eduardo Marban. CAPON modulates cardiac repolarization via neuronal nitric oxide synthase signaling in the heart. PNAS 2008, 105(11):4477-4482
4. Men Are More Susceptible Than Women to Methadone-Associated QTc Prolongation During Treatment for Heroin Dependence.

Kuan-Cheng Chang, Chieh-Liang Huang, Wen-Miin Liang, Li-Na Liao, and Hsien-Yuan Lane, submitted abstract for 2011 AHA meeting

[925] *CAPON,* a Nitric Oxide Synthase Regulator Associated with QT Interval Variation in Humans, Modulates Cardiac Repolarization in Ventricular Myocytes

Kuan-Cheng Chang, Andreas S. Barth, Eddy Kizana, Yuji Kashiwakura, Tetsuo Sasano, Yiqiang Zhang, Hee Cheol Cho, Ting Liu, Eduardo Marbán, Johns Hopkins Univ, Baltimore, MD

Background: A common genetic variant in a putative regulatory region of the neuronal nitric oxide synthase regulator *CAPON* gene has recently been associated with differences in the electrocardiographic QT interval in a human genome-wide study. As *CAPON* was previously unsuspected to play a role in the heart, we sought to identify *CAPON* in cardiomyocytes and characterize the biological effects of *CAPON* overexpression in cardiomyocytes.

Methods and Results: Endogenous expression of *CAPON* protein was documented by immunofluorescence microscopy of freshly-isolated guinea pig left ventricular (LV) cardiomyocytes and western blot analysis of LV myocardium. For patch-clamp studies, the *CAPON* cDNA was cloned from guinea pig LV myocardium and then subcloned into an adenoviral vector (Ad*CAPON*-GFP) coexpressing the reporter eGFP. *In vivo* gene transfer to the guinea pig heart was performed by direct injection of Ad*CAPON*-GFP into the LV apex. Action potential duration (APD) and ionic currents were recorded from cardiomyocytes isolated five days after viral transduction. In *CAPON*-transduced cardiomyocytes, the APD90 was shortened to 284 + 21 (n=8) and 240 + 8 (n=9) ms at 0.05 Hz and 1 Hz, respectively, compared to 383 + 25 (n=9) and 313 + 17 (n=12) in non-transduced myocytes (p=0.004 and 0.002, respectively). APD shortening was mediated by a reduction in peak L-type calcium current density in *CAPON*-transduced cardiomyocytes (-7.2 + 0.5 pA/pF, n=8), compared to the non-transduced cardiomyocytes (-11.2 + 1.0 pA/pF, n=12, p=0.006). Interestingly, there was also a reduction of delayed rectifier tail current density at -40 mV (1.1 + 0.1 pA/pF in *CAPON*-transduced cardiomyocytes (n=9), compared to 1.8 + 0.3 pA/pF (p=0.03) in non-transduced cardiomyocytes (n=10)), while current density of the inward rectifier was not changed.

Conclusions: We demonstrate endogenous *CAPON* protein expression in LV cardiomyocytes, and show that overexpression of this protein

accelerates cardiac repolarization via a reduction of L-type calcium current (which prevails over a concomitant reduction in IK). Our findings motivate the hypothesis that *CAPON* gene variants affect the expression level of *CAPON* protein in the heart and thereby influence cardiac repolarization.

K. Chang, None; **A. Barth**, None; **E. Kizana**, None; **Y. Kashiwakura**, None; **T. Sasano**, None; **Y. Zhang**, None; **H. Cho**, None; **T. Liu**, None; **E. Marbán**, None.

Session Info: Cellular Electrophysiology II - Tuesday, November 14, 2006, 09:00 AM-11:45 AM

Presentation Time: 9:15 AM

Room: McCormick Place, E353c

Circulation, 2006;114(18):II-167 (Supplement)

CAPON Interacts With Neuronal Nitric Oxide Synthase To Modulate L-type Calcium Current And Action Potential Duration In Ventricular Cardiomyocytes

Author Block: Kuan-Cheng Chang, Andreas S. Barth, Tetsuo Sasano, Yiqiang Zhang, Junichiro Miake, Eduardo Marbán, Johns Hopkins Univ, Baltimore, MD

Abstract:

Background: We have previously demonstrated expression of endogenous *CAPON* in heart and overexpression of *CAPON* resulting in shortening of action potential duration (APD) via reduction of ICa,L and increase of IKr. We hypothesized that the effects of *CAPON* overexpression are due to modifications of the NOS-NO pathways in the heart. Therefore, we sought to explore how *CAPON* interacts with NOS in ventricular myocytes (VM) and to dissect the mechanisms of *CAPON* overexpression-mediated changes in cellular electrophysiology.

Methods and Results: To probe protein-protein interaction of *CAPON* and NOS, normal guinea pig VM lysates were immunoprecipitated with *CAPON* antibody and probed by *CAPON*, nNOS and eNOS antibodies, respectively. We found that *CAPON*-nNOS, but not eNOS, exists as a physiological complex in VM. To explore how *CAPON* overexpression affects NOS, freshly isolated VM were *in vitro* transduced with an adenoviral vector (Ad*CAPON*-GFP), or the reporter only AdGFP, or not infected with any virus. After 40.3 ± 1.9 hours of cell culture, nNOS became hardly detectable in control VM with and without AdGFP transduction by western blot, whereas nNOS was preserved in the Ad*CAPON*-GFP transduced VM (n=3). We further imaged intracellular NO using DAR-4M AM in living VM isolated 3-5 days after *in vivo* gene transfer of *CAPON*. With 2 mM L-arginine, the NO fluorescence was increased in *CAPON*-overexpressed VM (1421 ± 28.2 au, n=43) compared to that of the control VM (1329 ± 19.1 au, n=166; $p<0.05$). In patch-clamp studies, in *CAPON*-overexpressed VM, the peak ICa,L density was smaller (-5.1 ± 0.9 pA/pF, n=14 vs. -6.5 ± 0.8 pA/pF, n=14; $p<0.001$) and the APD90 was shorter (221.6 ± 18.2 ms, n=6 vs. 333.7 ± 18.7 ms, n=7; $p<0.01$) than those of the control VM. Pretreatment with 1 mM L-NAME reversed the peak ICa,L density reduction (-6.2 ± 1.4 pA/pF, n=14 vs. -6.6 ± 1.3 pA/pF, n=14; p=NS) and the APD90 abbreviation (348.3 ± 44.2 ms, n=7 vs. 378.5 ± 44.8 ms, n=5; p=NS) in *CAPON*-overexpressed VM.

Conclusions: We demonstrate *CAPON*-nNOS protein-protein interaction in VM and find that overexpression of *CAPON* may upregulate the nNOS-NO pathway, thereby modulating ICa,L and APD. The findings provide a rationale for the association of *CAPON* gene variants with extremes of the QT interval in human populations.

***Circulation*, Oct 2007;116:II-11-12 (Supplement)**

Men Are More Susceptible Than Women to Methadone-Associated QTc Prolongation During Treatment for Heroin Dependence

Kuan-Cheng Chang, Chieh-Liang Huang, Wen-Miin Liang, Li-Na Liao, and Hsien-Yuan Lane China Medical University and the Hospital, Taichung, TAIWAN

Introduction: Methadone, a useful drug in the treatment of heroin dependence, is associated with dose-dependent QTc prolongation and sudden death in susceptible patients. Whether there is a gender difference in susceptibility to methadone-associated QTc prolongation remains unknown. Methods: To assess the gender effects on methadone-associated QTc prolongation in a cross-sectional manner, a total of 199 patients (aged 38±7 years; 160 men, 39 women) who received a standard digital 12-lead ECG examination after stable methadone treatment were recruited. For longitudinal evaluation, a separate population of 123 patients (aged 37±7 years; 101 men, 22 women) who underwent a 12-lead ECG before and 37±8 days after methadone treatment were enrolled. The QT interval was measured automatically by the Marquette 12SL based on a "Global Median" beat algorithm and corrected by heart rate using Bazett's formula. Results: In the cross-sectional study, a positive dose-dependent association was identified between QTc interval and methadone dose in men (Figure 1). However, this correlation was not significant in women (Figure 2). The longitudinal assessment for men revealed significant QTc lengthening (432.3±24.1 vs. 421.8±23.7 ms, p=0.0007) 37±9 days after methadone treatment (48.3±20.8 mg) compared to the baseline, while the change was not significant for women (427.4±19.4 vs. 441.3±47.3 ms, p=0.75) with equivalent methadone treatment duration (36±4 days) and dose (57.4±22.2 mg). Conclusions: Men appear to be more susceptible to methadone-associated QTc prolongation than women. The underlying mechanisms remain to be elucidated.

CAPON modulates cardiac repolarization via neuronal nitric oxide synthase signaling in the heart

Kuan-Cheng Chang*†, Andreas S. Barth*, Tetsuo Sasano*, Eddy Kizana*, Yuji Kashiwakura*, Yiqiang Zhang*, D. Brian Foster*, and Eduardo Marbán*‡§

*Institute of Molecular Cardiobiology, The Johns Hopkins University, Baltimore, MD 21205; †Graduate Institute of Clinical Medical Science, China Medical University and Hospital, Taichung 40447, Taiwan; and ‡Heart Institute, Cedars Sinai Medical Center, Los Angeles, CA 90048

Edited by Eric N. Olson, University of Texas Southwestern Medical Center, Dallas, TX, and approved January 10, 2008 (received for review September 26, 2007)

Congenital long- or short-QT syndrome may lead to life-threatening ventricular tachycardia and sudden cardiac death. Apart from the rare disease-causing mutations, common genetic variants in CAPON, a neuronal nitric oxide synthase (NOS1) regulator, have recently been associated with QT interval variations in a human whole-genome association study. CAPON had been unsuspected of playing a role in cardiac repolarization; indeed, its physiological role in the heart (if any) is unknown. To define the biological effects of CAPON in the heart, we investigated endogenous CAPON protein expression and protein–protein interactions in the heart and performed electrophysiological studies in isolated ventricular myocytes with and without CAPON overexpression. We find that CAPON protein is expressed in the heart and interacts with NOS1 to accelerate cardiac repolarization by inhibition of L-type calcium channel. Our findings provide a rationale for the association of CAPON gene variants with extremes of the QT interval in human populations.

NOS1 | QT interval | cardiac electrophysiology

Rare disease-causing mutations leading to congenital long- or short-QT syndrome are well recognized, but there is little insight into genetic sources of QT interval variation in normal populations. A whole-genome association approach has recently implicated common genetic variants in CAPON as contributing to QT interval differences in a community-based German population (1). This association has since been confirmed in other populations (2, 3). The genetic findings challenge our current understanding of QT physiology. CAPON, first identified in rat brain neurons (4), is a highly conserved protein (≈92% conceptual amino acid sequence identity between rat and human) with an N-terminal phosphotyrosine-binding (PTB) domain and a C-terminal PDZ-binding [postsynaptic density-95 (PSD95)/drosophila discs large/zona occludens-1] domain (4–6). In brain, CAPON competes with PSD95 for the binding of neuronal nitric oxide synthase (NOS1) through the interaction of its C terminus with the PDZ domain of NOS1 (4), thus uncoupling the NMDA–NOS1–NO-mediated signaling pathways. CAPON is also an adaptor protein of NOS1, capable of directing NOS1 to specific target proteins (5, 6). Nowhere, however, has CAPON been suspected of playing a role in cardiac physiology.

Both NOS1 and endothelial NOS (NOS3) are constitutively expressed in cardiomyocytes (7). NOS1 in the sarcolemma has been proposed to interact with Na^+-K^+ ATPase (8) and with the plasma membrane Ca^{2+}/calmodulin-dependent Ca^{2+} ATPase (PMCA) through the interaction of PDZ domain of NOS1 and the C terminus of PMCA4b isoform (9). In the sarcoplasmic reticulum (SR), NOS1 is structurally associated with ryanodine receptor 2 (RyR2) (10) and cardiac SR Ca^{2+} ATPase (SERCA2) (11) to regulate intracellular calcium cycling and excitation–contraction coupling. Conditional transgenic overexpression of NOS1 in heart leads to additional association of NOS1 and the sarcolemmal L-type calcium channel and thus suppresses the L-type calcium currents ($I_{Ca,L}$) (12). All of these lines of evidence highlight the notion that NOS1 plays a key role in regulating cardiac physiology.

Here, we hypothesized that CAPON is expressed in the heart and interacts with NOS1 to exert its biological effects. Therefore, we first sought to identify endogenous CAPON protein in ventricular myocytes and to characterize its physiological relevance by overexpression of CAPON using *in vivo* somatic gene transfer. We then probed the interaction between CAPON and the NOS–NO signaling pathways to dissect the potential mechanisms underlying the biological effects of CAPON in the heart.

Results

Identification of Endogenous CAPON Protein in the Heart. Because CAPON expression has not been documented in the heart, we first sought to probe the endogenous CAPON protein in guinea pig ventricular myocardium by Western blotting. The protein bands from guinea pig heart were compared with those from lung and brain tissues and from HEK293 cells with heterologous overexpression of CAPON by *in vitro* gene transfer with a bicistronic adenoviral vector (AdCAPON-GFP). The ventricular myocardium exhibited a band migrating near the 60-kDa marker, as expected for endogenous full-length CAPON, comparable with the comigration bands from HEK293 cells with heterologously overexpressed CAPON and from brain, which has abundant endogenous CAPON (Fig. 1*A*). The higher bands (≈70 kDa) could reflect either posttranslational modification of CAPON or nonspecific cross-reactivity. Notably, the ventricular myocardium also displayed a band ≈30 kDa in size detected by antibody against the C terminus of CAPON, but not by antibody against an N-terminal epitope, which is consistent with the short-form of CAPON (13). Immunofluorescent staining of freshly isolated ventricular myocytes revealed a cytoplasmic distribution pattern of the soluble CAPON protein with focal accentuation over the perinuclear region and the sarcolemmal membrane (Fig. 1*B*). Additionally, enhancement of CAPON immunofluorescence can be appreciated in CAPON-overexpressing myocytes. Therefore, expression of the endogenous CAPON protein in ventricular myocytes and overexpression of CAPON by AdCAPON-GFP-mediated gene transfer were both confirmed biochemically.

Adenovirus Alone Does Not Affect Electrophysiology. Both action potential duration (APD) and peak $I_{Ca,L}$ density were equivalent between AdGFP-transduced and nontransduced myocytes (Fig. 2

Author contributions: E.M. designed research; K.-C.C., A.S.B., T.S., E.K., Y.K., and Y.Z. performed research; T.S., E.K., Y.K., and D.B.F. contributed new reagents/analytic tools; K.-C.C., A.S.B., T.S., E.K., Y.K., Y.Z., D.B.F., and E.M. analyzed data; and K.-C.C., A.S.B., and E.M. wrote the paper.

The authors declare no conflict of interest.

This article is a PNAS Direct Submission.

§To whom correspondence should be addressed. E-mail: eduardo.marban@csmc.edu.

This article contains supporting information online at www.pnas.org/cgi/content/full/0709118105/DC1.

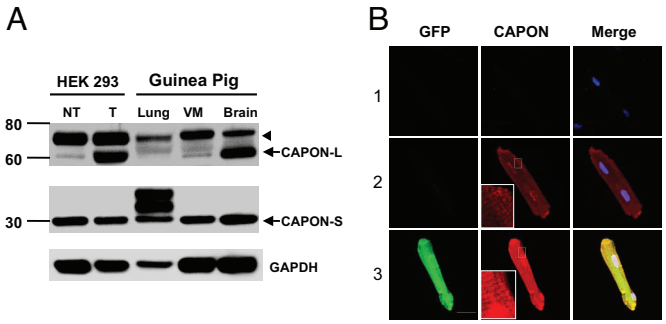

Fig. 1. Identification of endogenous CAPON protein in the heart. (*A*) Tissue homogenates from normal guinea pig ventricular myocardium (VM), brain, and lung, and HEK293 cells with (T) and without (NT) *in vitro* transduction with AdCAPON-GFP were subjected to SDS/PAGE Western blotting. Both full-length (CAPON-L) and short-form of CAPON (CAPON-S) are expressed in VM. The higher bands (arrowhead) could be caused by either posttranslational modification of CAPON or nonspecific cross-reactivity. (*B*) Immunostaining of CAPON in AdCAPON-GFP-transduced (3) and nontransduced (2) ventricular myocytes. Negative controls (secondary antibody only) are depicted in 1.

A and *B*). See supporting information (SI) *Results* for details. After ascertaining that adenoviral transduction alone does not alter cellular electrophysiology, we examined the effects of CAPON overexpression by comparing the electrophysiological parameters between AdCAPON-GFP-transduced and nontransduced myocytes.

CAPON Overexpression Accelerates Action Potential. To determine whether CAPON modulates cardiac repolarization, we compared the APD in freshly isolated control and CAPON-overexpressing ventricular myocytes at 1, 2, and 0.05 Hz. At 1-Hz stimulation, the mean APD_{10}, APD_{50}, APD_{75}, and APD_{90} were significantly shortened to 54.0 ± 7.2, 198.8 ± 8.1, 221.8 ± 7.9, and 233.9 ± 7.7 ms in CAPON-overexpressing cardiomyocytes ($n = 9$) compared with 96.6 ± 11.5, 291.0 ± 16.4, 316.1 ± 17.2, and 327.5 ± 17.9 ms in control myocytes ($n = 13$, $P < 0.05$, respectively) (Fig. 2 *C–E*). The abbreviation of APD with CAPON overexpression was maintained at 2 Hz and 0.05 Hz (data not shown), and the magnitude of APD_{90} reduction by CAPON overexpression was 28.6% at 1-Hz stimulation. We next explored the ionic basis for the abbreviation of APD.

L-Type Calcium Current. In CAPON-overexpressing myocytes, the peak $I_{Ca,L}$ density was significantly reduced (−7.2 ± 0.5 pA/pF, at +20 mV, $n = 8$) compared with that of control myocytes (−11.0 ± 1.0 pA/pF, at +10 mV, $n = 12$; $P < 0.05$) (Fig. 2 *F* and *G*). The reduction of the peak $I_{Ca,L}$ density was 35% (Fig. 2*G*). Averaged peak current density–voltage relationships revealed significant suppression of peak $I_{Ca,L}$ density from −30 mV to +40 mV ($P < 0.05$, respectively) by CAPON overexpression (Fig. 2*H*). By a decrease in net inward current, the CAPON-induced inhibition of peak $I_{Ca,L}$ density would contribute to the abbreviation of APD.

Sodium Current. Sodium current (I_{Na}) was not affected by CAPON overexpression (Fig. 3 *A* and *B*). For details see *SI Results*.

Outward Rectifier Potassium Current. In guinea pig ventricular myocytes, there are two types of delayed rectifier potassium currents, the rapidly activating component (I_{Kr}) and the slowly activating component (I_{Ks}) (14), responsible for terminating the action potential plateau. To probe the potential contribution of these currents to CAPON overexpression-mediated APD changes, we first recorded the total I_K tail currents and then used a specific I_{Ks} blocker, chromanol 293B (15), to separate I_{Kr} and I_{Ks} in CAPON-overexpressing and control myocytes. Although neither the total I_K nor the I_{Ks} tail current density was changed between nontransduced control and CAPON-overexpressing myocytes, we found the I_{Kr} peak tail current density to be modestly enhanced in CAPON-overexpressing myocytes (0.92 ± 0.07 pA/pF, $n = 10$) compared with control myocytes (0.61 ± 0.08 pA/pF, $n = 7$; $P < 0.05$) (Fig. 3 *C* and *D*). These results indicate that in addition to the reduction of $I_{Ca,L}$, enhancement of I_{Kr} also contributes to the abbreviation of APD in CAPON-overexpressing myocytes.

Inward Rectifier Potassium Current. Inward rectifier potassium current (I_{K1}) was not changed by CAPON overexpression (Fig. 3*E*). See *SI Results* for details.

Protein–Protein Interaction of CAPON and NOS1 in the Heart. After identifying that both full-length and short-form CAPON proteins are expressed in the heart and overexpression of CAPON accelerates APD by suppression of $I_{Ca,L}$ and augmentation of I_{Kr}, the important next step is to answer whether the electrophysiological changes induced by CAPON overexpression were caused by modifications of the NOS–NO pathways. First, we determined whether

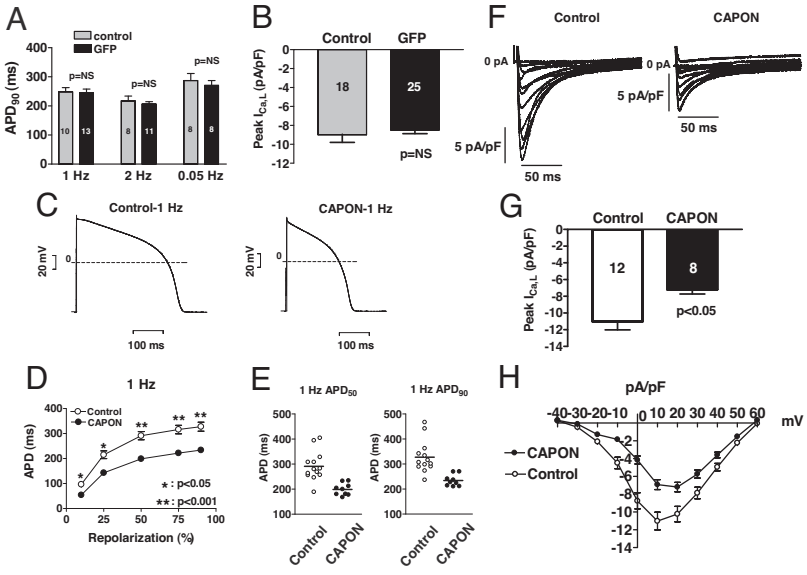

Fig. 2. Electrophysiological effects of CAPON overexpression in guinea pig ventricular myocytes. (*A* and *B*) Adenovirus alone does not affect electrophysiology. For details, see *SI Results*. (*C–H*) CAPON overexpression abbreviates the action potential duration and reduces $I_{Ca,L}$. (*C*) APD was markedly shortened in a representative AdCAPON-GFP-transduced myocyte compared with a representative control myocyte. (*D*) Significant abbreviation of APD can be seen spanning from APD_{10} to APD_{90} at 1-Hz stimulation in CAPON-overexpressing myocytes (CAPON, $n = 9$; control, $n = 13$). (*E*) The actual APD_{50} and APD_{90} measured from individual myocyte comprising each group reveal a consistent reduction of APD in CAPON-overexpressing myocytes. (*F*) Representative $I_{Ca,L}$ recordings elicited by depolarizing voltage steps (500 ms) from −40 to +60 mV in 10-mV increments after a prepulse from −80 mV to −40 mV show reduction of $I_{Ca,L}$ in a AdCAPON-GFP-transduced myocyte compared with a control myocyte. (*G*) The peak $I_{Ca,L}$ density in CAPON-overexpressing myocytes was smaller than in control myocytes. (*H*) Averaged peak current–voltage relationships demonstrate attenuation of $I_{Ca,L}$ at multiple depolarizing pulses in CAPON-overexpressing myocytes (CAPON, $n = 8$; control, $n = 12$). The number inside each bar graph indicates the number of cells studied.

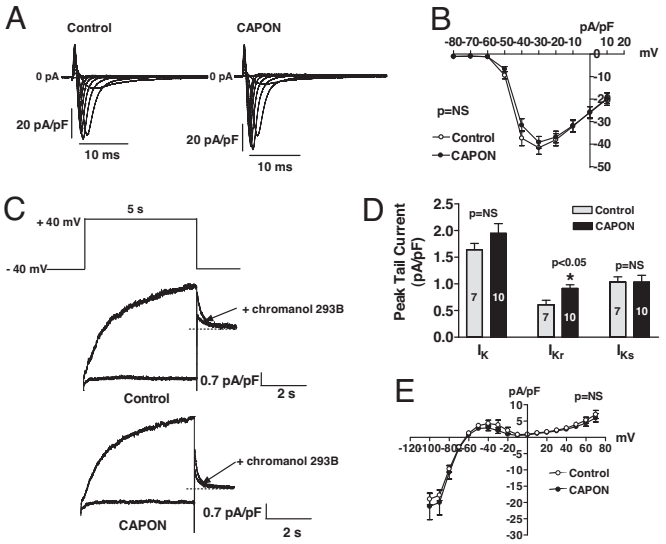

Fig. 3. Electrophysiological effects of CAPON overexpression in guinea pig ventricular myocytes. (*A* and *B*) CAPON overexpression does not affect sodium current. For more details, see *SI Results*. (*C–E*) CAPON overexpression enhances I_{Kr}. (*C*) Delayed rectifier K^+ tail current was measured in response to a depolarizing pulse to +40 mV for 5 s followed by repolarization to −40 mV. I_{Kr} was recorded after steady-state suppression of I_{Ks} by chromanol 293B. Representative recordings show a larger I_{Kr} tail current in a CAPON-overexpressing myocyte compared with a control myocyte. (*D*) Neither peak I_K nor I_{Ks} tail current densities were significantly different between CAPON-overexpressing and control myocytes. However, peak I_{Kr} tail current density was modestly enhanced in CAPON-overexpressing myocytes. (*E*) Instantaneous I_{K1} current density elicited by ramp protocol from −100 to + 70 mV (5 s) was not different between CAPON-overexpressing (n = 10) and control myocytes (n = 9).

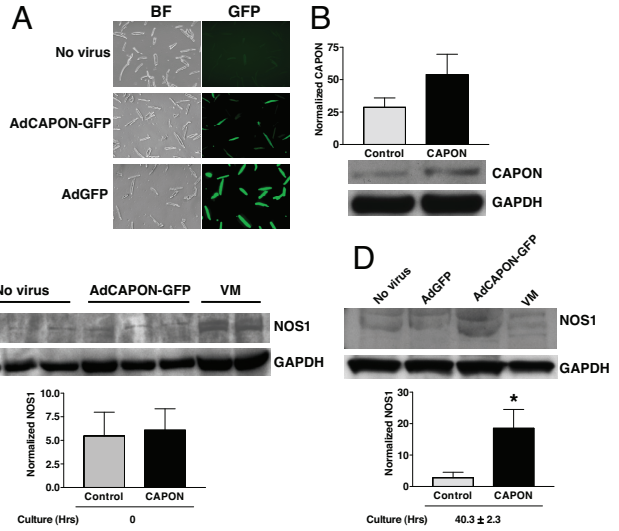

Fig. 5. CAPON overexpression stabilizes NOS1 in ventricular myocytes. (*A*) Freshly isolated ventricular myocytes were transduced *in vitro* with AdCAPON-GFP, or AdGFP, or not transduced with either virus. BF, bright-field microscopic images. (*B*) The *in vitro* AdCAPON-GFP transduction caused a 1.9-fold increase of the CAPON level. (*C*) At 0 h of culture, the NOS1 level was not different between AdCAPON-GFP-transduced and nontransduced myocytes (n = 3 animals). (*D*) After 40.3 ± 2.3 h of cell culture, NOS1 became down-regulated in both ventricular myocytes transduced with AdGFP and in nontransduced myocytes, whereas NOS1 was well preserved in the AdCAPON-GFP-transduced ventricular myocytes. The mean NOS1 level from nontransduced and AdGFP-transduced myocytes was lower than that of AdCAPON-GFP-transduced myocytes (*, $P < 0.05$ vs. control, n = 3 animals). Noncultured ventricular tissue homogenates (VM) served as positive control for NOS1 detection. The signal intensities of CAPON and NOS1 are normalized against the GAPDH signals.

CAPON interacts with NOS in the heart. To assess protein–protein interactions of CAPON and NOS, normal guinea pig ventricular tissue homogenates were immunoprecipitated with anti-CAPON- or anti-NOS1-bound protein G complex, separated by SDS/PAGE, and probed by CAPON, NOS1, and NOS3 antibodies, respectively. The crude tissue homogenates served as the positive controls while probing NOS1, NOS3, and CAPON (Fig. 4). We found that NOS1 specifically coimmunoprecipitated with the bound CAPON antibodies (Fig. 4 *A* and *B*), whereas NOS3 was not detected in the anti-CAPON immunoprecipitates (Fig. 4 *C* and *D*). To include a negative control, the ventricular myocardial homogenates were also incubated overnight with the protein G complex without prebound CAPON antibody; as a result, neither NOS1 nor CAPON could be detected in the eluted precipitates (Fig. 4 *A* and *B*). These findings indicate that CAPON–NOS1, but not CAPON–NOS3, exists as a physiological complex in ventricular myocytes.

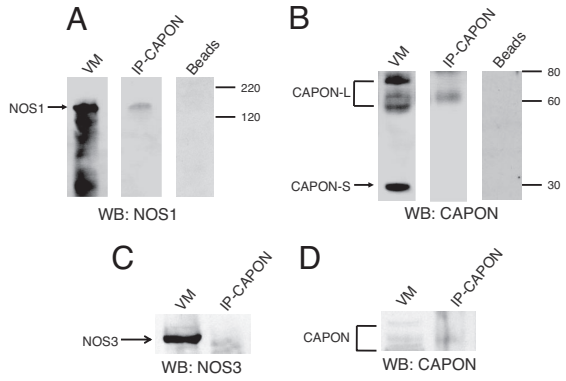

Fig. 4. CAPON interacts with NOS1, but not NOS3, in ventricular myocytes. Normal guinea pig ventricular tissue homogenates were immunoprecipitated overnight with anti-CAPON-bound protein G complex, separated by SDS/PAGE, and probed by anti-NOS1 (*A*), anti-CAPON (*B* and *D*), and anti-NOS3 (*C*), respectively. To include a negative control, the ventricular tissue homogenates were also incubated overnight with anti-CAPON-free protein G complex (beads). As a result, neither NOS1 nor CAPON could be detected in the eluted precipitates. WB, Western blotting.

CAPON Overexpression Stabilizes NOS1. Because CAPON interacts with NOS1 in the heart, we next wanted to know how CAPON overexpression affects NOS1 protein level and activity. Freshly isolated ventricular myocytes were transduced *in vitro* with AdCAPON-GFP, or AdGFP, or not transduced with either virus. The gene transfer efficiency was confirmed by ≈100% GFP-positive cells in AdGFP-transduced myocytes and ≈50% GFP positive cells in AdCAPON-GFP myocytes, compared with only background autofluorescence (i.e., 0% GFP positivity) in nontransduced myocytes (Fig. 5*A*). The *in vitro* AdCAPON-GFP transduction caused a 1.9-fold increase of the CAPON protein level (Fig. 5*B*). At 0 h of culture, the NOS1 level was not different between AdCAPON-GFP-transduced and nontransduced myocytes (5.47 ± 2.51% vs. 6.08 ± 2.27%, n = 3 animals; p = NS) (Fig. 5*C*). After 40.3 ± 2.3 h of cell culture, NOS1 was down-regulated in nontransduced and AdGFP-transduced myocytes but was up-regulated in AdCAPON-GFP-transduced myocytes. Therefore, the mean NOS1 level from nontransduced and AdGFP-transduced myocytes was lower than that of AdCAPON-GFP-transduced myocytes (2.78 ± 1.75% vs. 18.54 ± 5.99%; $P < 0.05$) (Fig. 5*D*). Of note, NOS3 protein levels were not changed in AdCAPON-GFP-transduced myocytes (data not shown). Noncultured ventricular tissue homogenates served as positive control for the NOS1/NOS3

PHYSIOLOGY

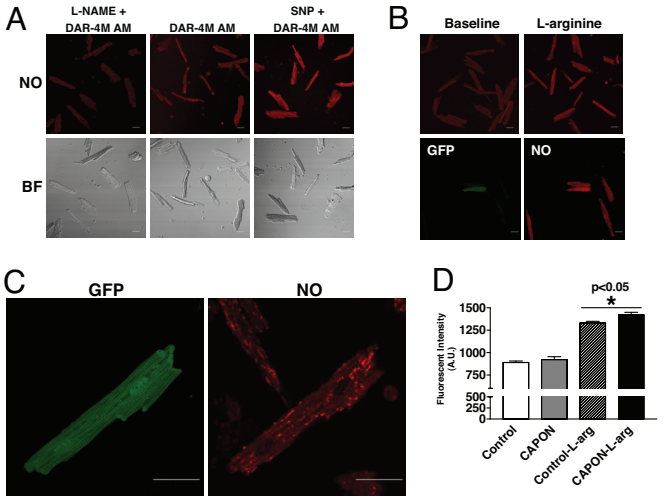

Fig. 6. Enhanced intracellular NO production in CAPON-overexpressing myocytes. (*A*) The specificity of DAR-4M AM was verified by a differential fluorescent intensity with the addition of SNP or L-NAME. (*B*) The NO fluorescence was enhanced after L-arginine stimulation. In GFP (+), CAPON-overexpressing myocytes, the NO fluorescence was stronger than in control myocytes. (*C*) Representative high-powered images illustrate a modest enhancement of the NO fluorescent marker in a CAPON-overexpressing myocyte. (*D*) The baseline fluorescent intensity was equivalent in CAPON-overexpressing (n = 30) and control myocytes (n = 90), whereas with the addition of L-arginine, the fluorescence intensity increased disproportionately in CAPON-overexpressing myocytes (CAPON-L-arg) (n = 43) compared with controls (Control-L-arg) (n = 166).

expression assays. These findings suggest that CAPON overexpression may stabilize NOS1 in ventricular myocytes.

Enhanced Intracellular NO Production in CAPON-Overexpressing Myocytes. Because NO generation reflects NOS activity, we further imaged intracellular NO production by using a rhodamine-based chromophore, DAR-4M AM, in living ventricular myocytes isolated 3–5 days after *in vivo* gene transfer of CAPON. To test the specificity of DAR-4M AM for NO imaging, we measured fluorescence intensity in ventricular myocytes loaded with DAR-4M AM only or DAR-4M AM + sodium nitroprusside (SNP) or DAR-4M AM + N^G-nitro-L-arginine methyl ester (L-NAME). Fluorescence intensified with the addition of SNP and waned with L-NAME compared with that in myocytes incubated with DAR-4M AM only (Fig. 6*A*). Next, we compared NO production between CAPON-overexpressing myocytes and control myocytes incubated with DAR-4M AM only or DAR-4M AM + 2 mM L-arginine (Fig. 6 *B–D*). The baseline fluorescent intensity was equivalent in CAPON-overexpressing and control myocytes (921.6 ± 32.5 a.u., n = 30 vs. 888.6 ± 17.3 a.u., n = 90; P = NS), whereas with the addition of L-arginine, the fluorescence intensity increased disproportionately in CAPON-overexpressing myocytes (1,420.9 ± 28.1 a.u., n = 43) compared with controls (1,329.0 ± 19.1 a.u., n = 166; $P < 0.05$) (Fig. 6*D*). These results indicate that CAPON overexpression may enhance intracellular NO production, particularly in the presence of additional NOS substrates.

L-NAME Reverses CAPON Overexpression-Mediated APD Abbreviation and $I_{Ca,L}$ Reduction. After ascertaining that CAPON overexpression resulted in up-regulation of NOS1–NO activity, we examined the effects of L-NAME on $I_{Ca,L}$ and APD in ventricular myocytes isolated 3–5 days after *in vivo* gene transfer of CAPON. Pretreatment with 1 mM L-NAME reversed the APD_{90} abbreviation (1 Hz, 348.3 ± 47.8 ms, n = 7 vs. 378.5 ± 50.1 ms, n = 5; P = NS) (Fig. 7 *A* and *B*) and the $I_{Ca,L}$ density reduction (−6.2 ± 0.6 pA/pF, n = 14 vs. −6.6 ± 0.4 pA/pF, n = 14; P = NS) (Fig. 7 *C–E*) in CAPON-overexpressing ventricular myocytes. Interestingly, APD_{90} tends to become longer (378.5 ± 50.1 ms, n = 5 vs. 333.7 ± 20.2 ms, n = 7; P = NS) (Fig. 7 *A* and *B*), and the peak $I_{Ca,L}$ density tends to increase, too (−6.6 ± 0.4 pA/pF, n = 14 vs. −6.3 ± 0.3 pA/pF, n = 14; P = NS) (Fig. 7 *C–E*) in control myocytes after pretreatment with L-NAME. However, these changes were not statistically significant. In contrast, significant lengthening of APD_{90} (1 Hz, 348.3 ± 47.8 ms, n = 7 vs. 221.6 ± 19.9 ms, n = 6; $P < 0.05$) (Fig. 7 *A* and *B*) and the increase of the peak $I_{Ca,L}$ density (−6.2 ± 0.6 pA/pF, n = 14 vs. −4.8 ± 0.3 pA/pF, n = 14; $P < 0.05$) (Fig. 7 *C–E*) were only seen in CAPON-overexpressing myocytes after pretreatment with L-NAME.

Discussion

We demonstrate that CAPON, the brain-enriched NOS1 adaptor/regulator protein, is expressed in the heart and interacts with NOS1.

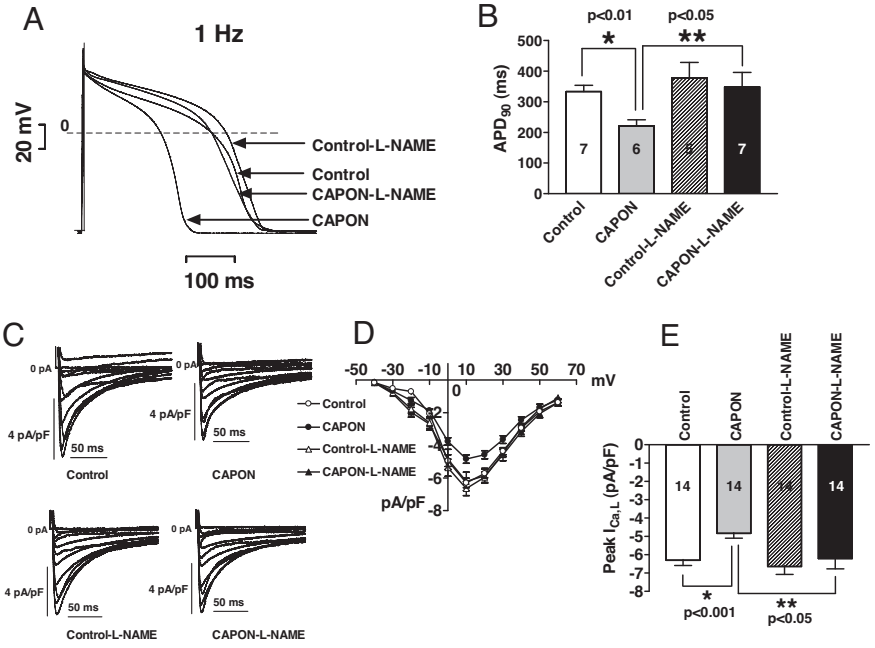

Fig. 7. L-NAME reverses CAPON overexpression-mediated APD abbreviation and $I_{Ca,L}$ reduction. (*A*) Representative action potential recordings show reversal of APD abbreviation with L-NAME in a CAPON-overexpressing myocyte. (*B*) Pretreatment with L-NAME significantly increased APD_{90} and reversed APD abbreviation in CAPON-overexpressing ventricular myocytes, whereas the APD90 was not significantly changed with L-NAME in control myocytes. (*C*) Representative $I_{Ca,L}$ recordings show reversal of $I_{Ca,L}$ suppression with L-NAME in a CAPON-overexpressing myocyte. (*D*) Averaged peak current–voltage relationships reveal significant increase of peak $I_{Ca,L}$ densities with L-NAME in CAPON-overexpressing myocytes but not in control myocytes. The number of cells studied in each group is indicated in bar graphs in *E*. (*E*) Pretreatment with L-NAME significantly increased peak $I_{Ca,L}$ density and rescued $I_{Ca,L}$ suppression in CAPON-overexpressing myocytes, whereas the peak $I_{Ca,L}$ density was not significantly changed with L-NAME in control myocytes.

Overexpression of CAPON results in up-regulation of the NOS1–NO signaling pathways, which further leads to abbreviation of APD through the inhibition of $I_{Ca,L}$ and enhancement of I_{Kr}.

Expression of Endogenous CAPON Protein in the Heart. Since the first identification of CAPON protein in the rat brain (4), Xu *et al*. (13) further found that CAPON protein has two isoforms that are translated from a full-length and a C-terminal splicing variant (13). The full-length transcript encompassing 10 exons contains both PTB- and PDZ-binding domains, whereas the C-terminal transcript containing the last 2 exons encodes only the PDZ-binding domain (13). We found that both full-length and short CAPON isoforms are expressed in guinea pig ventricular myocytes using the same CAPON antibody (13) predicted to react with the C terminus of CAPON. The full-length isoform comigrated at the same level as a brain-enriched protein band and a band from HEK293 cells expressing CAPON. Immunostaining reveals a cytoplasmic distribution of CAPON with focal accentuation around the perinuclear region and the cell membrane.

CAPON Overexpression Up-Regulates NOS1–NO Pathways. Given that CAPON acts as a regulator and adaptor of NOS1 in brain, we speculated that the CAPON overexpression-induced electrophysiological changes may be mediated by modifications of NOS–NO signaling pathways. To investigate this hypothesis, we began by probing the interactions of CAPON and NOS1 in the heart. We found that CAPON interacts with NOS1, but not NOS3, to form a physiological complex in guinea pig ventricular myocytes. This interaction was further supported by an intracellular colocalization of CAPON and NOS1 by immunostaining and confocal microscopy (SI Fig. 8). Interestingly, only the full-length CAPON isoform is responsible for the interaction with NOS1, because only a single full-length CAPON band (≈60 kDa) was detected in the eluted immunoprecipitates. These findings are in line with the previous observations that the full-length CAPON of a similar molecular mass was accountable for the interactions with NOS1 in neurons (4).

To explore how CAPON overexpression affects NOS1, we compared NOS1 protein level in cultured guinea pig ventricular nontransduced or AdGFP- or AdCAPON-GFP-transduced myocytes. Interestingly, the NOS1 protein becomes down-regulated both in ventricular myocytes transduced with AdGFP and in nontransduced myocytes, whereas NOS1 levels were well preserved in AdCAPON-GFP-transduced ventricular myocytes after 40 h of cell culture. However, NOS3 protein level was not obviously affected by AdCAPON-GFP transduction compared with control myocytes. This finding provides direct evidence to support the notion that CAPON has a functional role in stabilizing NOS1 in ventricular cardiomyocytes.

Because intracellular NO production directly reflects NOS activity, we further compared the intracellular NO generation between AdCAPON-GFP-transduced ventricular myocytes and nontransduced myocytes by using DAR-4M AM. The baseline intracellular NO production was equivalent between CAPON-overexpressing ventricular myocytes and control myocytes; however, with the addition of L-arginine, CAPON-overexpressing myocytes generated more NO than did the controls. Therefore, overexpression of CAPON in ventricular myocytes not only stabilizes NOS1 but may also enhance NOS1 activity. The absolute increase in NO production was only modest in CAPON-overexpressing compared with control myocytes (7%), yet it has to be kept in mind that these small but significant increases in global NO production may translate into biologically relevant local NO concentrations. Given the very short elimination half-life of NO, the biological effects of NOS1–NO signaling depend largely on the subcellular localization of NOS1, where CAPON might play a role to direct NOS1 to the specific target proteins. In addition, CAPON may compete with other PDZ-binding proteins for the PDZ domain. Therefore, it is possible that CAPON may exert its biological effects by mechanisms other than modulation of the NOS1–NO pathway.

CAPON Overexpression Shortens APD by Suppression of $I_{Ca,L}$ and Enhancement of I_{Kr}. The electrophysiological studies revealed that CAPON overexpression resulted in abbreviation of APD mediated by a diminished $I_{Ca,L}$ and an enhanced I_{Kr}. Because guinea pig ventricular myocytes lack endogenous I_{to} (16), $I_{Ca,L}$ and I_K represent the two principal currents controlling the length of the action potential plateau and APD. Accordingly, a 35% decrease of $I_{Ca,L}$ combined with a 50% increase in I_{Kr} is sufficient to explain the 30% shortening of APD_{90} observed with CAPON overexpression.

Reversal of CAPON Overexpression-Induced Electrophysiological Changes by L-NAME. Because we found that overexpression of CAPON stabilizes NOS1 and enhances NOS1-derived NO production, pharmacological intervention with a NOS blocker should be able to counteract CAPON overexpression-mediated electrophysiological changes. As expected, pretreatment with L-NAME significantly increased APD_{90} and $I_{Ca,L}$, thereby reversing APD abbreviation and $I_{Ca,L}$ suppression in CAPON-overexpressing ventricular myocytes. The magnitudes of increments in APD_{90} (57% vs. 13%) and $I_{Ca,L}$ (29% vs. 5%) in CAPON-overexpressing ventricular myocytes obviously surpass those of the control myocytes when both are exposed to L-NAME, excluding the possibility that a significant background effect of L-NAME is responsible for the changes. The differential electrophysiological responsiveness to L-NAME between CAPON-overexpressing myocytes and control myocytes further supports the notion that CAPON overexpression activates the NOS1–NO pathway to modulate cellular electrophysiology.

In guinea pig ventricular myocytes, NO can shorten APD by suppression of $I_{Ca,L}$ and augmentation of I_{Ks} (17, 18). The inhibition of $I_{Ca,L}$ by NO is caused by cGMP-dependent or cGMP-independent (direct *S*-nitrosylation/redox) pathways (17, 19, 20). Similarly, NO can modulate the delayed rectifier K^+ currents by cGMP-dependent or -independent pathway (17, 18, 21). Interestingly, although CAPON overexpression activates NOS1-derived NO in our work, the electrophysiological changes mediated by this NO activation are comparable with those in previous reports (17–19, 21). Recently, evidence emerged that NOS1 may play a critical role in the regulation of calcium handling and myocyte contraction in the heart (9, 10, 12, 22). Burkard *et al*. (12) observed that in a conditional NOS1-overexpressing transgenic mouse model, the peak $I_{Ca,L}$ density was significantly reduced by 39% in NOS1-overexpressing ventricular myocytes, which was attributed to the translocation of NOS1 to sarcolemma where NOS1 interacted with L-type calcium channel and caused inhibition of $I_{Ca,L}$. Conceivably, the observation that activated NOS1 is translocated to the sarcolemma where it interacts with ion channels may help explain our finding of $I_{Ca,L}$ inhibition and I_{Kr} augmentation.

In conclusion, CAPON protein is expressed in the heart and interacts with NOS1 to exert its biological effects. Overexpression of CAPON may stabilize NOS1 and activate NOS1-derived NO signaling cascades to shorten action potential duration via inhibition of L-type calcium channels and activation of delayed rectifier potassium channels. Our findings provide a rationale for the association of CAPON gene variants with extremes of the QT interval in human populations. Specifically, we propose that CAPON gene variants, which are in noncoding regions (1–3), act by influencing the basal expression level of CAPON in the heart, thereby affecting cardiac repolarization and the QT interval by the mechanisms identified here.

Study Limitations. In addition to the study of sarcolemmal ion channels, we did not examine the role of CAPON on calcium transients and excitation–contraction coupling in myocardium.

This investigation might be of particular importance, because NOS1–NO pathways have recently been related to play a role in regulating cardiac contractility (9, 10, 12). Moreover, because CAPON may compete with other PDZ-binding proteins for PDZ binding, it is likely that CAPON, in addition to modulating the NOS1–NO pathway, might also have other biological effects, particularly regarding stabilization of cell membrane proteins, including ion channels. Therefore, the changes in electrophysiology might be attributed not only to NO-dependent mechanisms (as laid out in the present work), but also to NO-independent mechanisms that have not been addressed herein. Finally, our experimental design did not allow us to examine the ECG phenotype in CAPON-overexpressing animals because only a small area of the left ventricular myocardium was injected, and the transduction efficiency was in the range of 1–10%. Therefore, our approach only allowed us to study changes in cellular electrophysiology, but not the global ECG phenotype. Future studies using transgenic models with CAPON overexpression and knockdown are needed to address this question.

Methods

This work conformed to the standards of the National Institutes of Health regarding care and use of laboratory animals and was performed in accordance with the guidelines of Animal Care and Use Committee of The Johns Hopkins University.

Cloning of CAPON cDNA, Plasmid Construction, and Adenovirus Preparation. The full-length CAPON cDNA was cloned from guinea pig ventricular myocardium and subcloned into a bicistronic adenoviral vector (AdCAPON-GFP) coexpressing the reporter GFP. For details see *SI Methods*.

Western Blot Analysis. To probe endogenous CAPON protein expression, tissue homogenates from normal guinea pig ventricular myocardium, brain, and lung and HEK293 cells with and without *in vitro* transduction with AdCAPON-GFP were subjected to SDS/PAGE Western blotting. See *SI Methods* for further details.

Coimmunoprecipitation of CAPON and NOS. Normal guinea pig ventricular tissue homogenates were immunoprecipitated overnight with anti-CAPON-bound protein G complex, separated by SDS/PAGE, and probed by anti-NOS1, anti-CAPON, and anti-NOS3, respectively. Further details are described in *SI Methods*.

Cell Culture and *in Vitro* Gene Transfer. For details, see *SI Methods*.

Immunofluorescent Staining and Confocal Microscopic Imaging. For details, see *SI Methods*.

***In Vivo* Gene Transfer and Myocyte Isolation.** *In vivo* gene transfer was performed by open-chest intramyocardial injection of the adenoviral vectors into the left ventricular apex. The ventricular myocytes were isolated 72 h after gene transfer for further studies. For details, see *SI Methods*.

Electrophysiological and Pharmacological Studies. Recording techniques and conditions are described in *SI Methods*.

Intracellular NO Imaging with DAR-4M AM. Intracellular NO production was imaged by DAR-4M AM in living ventricular myocytes isolated 3–5 days after *in vivo* transduction with AdCAPON-GFP. For further details, see *SI Methods*.

Statistical Analysis. All data are expressed as mean ± SEM. Comparison between groups was performed by using the unpaired Student's *t* test, and P values <0.05 were considered statistically significant.

ACKNOWLEDGMENTS. This work was supported in part by a grant from the Donald W. Reynolds Cardiovascular Clinical Research Center and by a Transatlantic Network of Excellence grant from the Le Ducq Foundation. K.-C.C. was supported by a research grant from China Medical University Hospital, Taichung, Taiwan; A.S.B. was supported by German Research Foundation (DFG) Grant BA 3341/1-1; and Y.Z. was supported by a Research Fellowship from the Heart and Stroke Foundation of Canada.

1. Arking D-E, *et al.* (2006) A common genetic variant in the NOS1 regulator NOS1AP modulates cardiac repolarization. *Nat Genet* 38:644–651.
2. Post W, *et al.* (2007) Associations between genetic variants in the NOS1AP (CAPON) gene and cardiac repolarization in the old order Amish. *Hum Hered* 64:214–219.
3. Aarnoudse A-J, *et al.* (2007) Common NOS1AP variants are associated with a prolonged QTc interval in the Rotterdam study. *Circulation* 116:10–16.
4. Jaffrey S-R, Snowman A-M, Eliasson M-J, Cohen N-A, Snyder S-H (1998) CAPON: A protein associated with neuronal nitric oxide synthase that regulates its interactions with PSD95. *Neuron* 20:115–124.
5. Fang M, *et al.* (2000) Dexras1: A G protein specifically coupled to neuronal nitric oxide synthase via CAPON. *Neuron* 28:183–193.
6. Jaffrey S-R, Benfenati F, Snowman A-M, Czernik A-J, Snyder S-H (2002) Neuronal nitric-oxide synthase localization mediated by a ternary complex with synapsin and CAPON. *Proc Natl Acad Sci USA* 99:3199–3204.
7. Hare J-M, Stamler J-S (2005) NO/redox disequilibrium in the failing heart and cardiovascular system. *J Clin Invest* 115:509–517.
8. Xu K-Y, *et al.* (2003) Nitric oxide protects cardiac sarcolemmal membrane enzyme function and ion active transport against ischemia-induced inactivation. *J Biol Chem* 278:41798–41803.
9. Oceandy D, *et al.* (2007) Neuronal nitric oxide synthase signaling in the heart is regulated by the sarcolemmal calcium pump 4b. *Circulation* 115:483–492.
10. Barouch L-A, *et al.* (2002) Nitric oxide regulates the heart by spatial confinement of nitric oxide synthase isoforms. *Nature* 416:337–340.
11. Xu K-Y, Huso D-L, Dawson T-M, Bredt D-S, Becker L-C (1999) Nitric oxide synthase in cardiac sarcoplasmic reticulum. *Proc Natl Acad Sci USA* 96:657–662.
12. Burkard N, *et al.* (2007) Conditional neuronal nitric oxide synthase overexpression impairs myocardial contractility. *Circ Res* 100:e32–e44.
13. Xu B, *et al.* (2005) Increased expression in dorsolateral prefrontal cortex of CAPON in schizophrenia and bipolar disorder. *PLoS Med* 2:999–1007.
14. Sanguinetti M-C, Jurkiewicz N-K (1990) Two components of cardiac delayed rectifier K^+ current: Differential sensitivity to block by class III antiarrhythmic agents. *J Gen Physiol* 96:195–215.
15. Bosch R-F, *et al.* (1998) Effects of the chromanol 293B, a selective blocker of the slow, component of the delayed rectifier K^+ current, on repolarization in human and guinea pig ventricular myocytes. *Cardiovasc Res* 38:441–450.
16. Inoue M, Imanaga I (1993) Masking of A-type K^+ channel in guinea pig cardiac cells by extracellular Ca^{2+}. *Am J Physiol* 264:C1434–C1438.
17. Bai C-X, Takahashi K, Masumiya H, Sawanobori T, Furukawa T (2004) Nitric oxide-dependent modulation of the delayed rectifier K^+ current and the L-type Ca^{2+} current by ginsenoside Re, an ingredient of *Panax ginseng*, in guinea pig cardiomyocytes. *Br J Pharmacol* 142:567–575.
18. Bai C-X, *et al.* (2005) Role of nitric oxide in Ca^{2+} sensitivity of the slowly activating delayed rectifier K^+ current in cardiac myocytes. *Circ Res* 96:64–72.
19. Campbell D-L, Stamler J-S, Strauss H-C (1996) Redox modulation of L-type calcium channels in ferret ventricular myocytes: Dual mechanism regulation by nitric oxide and *S*-nitrosothiols. *J Gen Physiol* 108:277–293.
20. Furukawa T, *et al.* (2006) Ginsenoside Re, a main phytosterol of *Panax ginseng*, activates cardiac potassium channels via a nongenomic pathway of sex hormones. *Mol Pharmacol* 70:1916–1924.
21. Han N-L, Ye J-S, Yu A, Sheu F-S (2006) Differential mechanisms underlying the modulation of delayed-rectifier K^+ channel in mouse neocortical neurons by nitric oxide. *J Neurophysiol* 95:2167–2178.
22. Sears C-E, *et al.* (2003) Cardiac neuronal nitric oxide synthase isoform regulates myocardial contraction and calcium handling. *Circ Res* 92:e52–e59.